Comptes Rendus

Chimie

Paul-Gabriel Julliard, Simon Pascal, Olivier Siri, Diego Cortés-Arriagada, Luis Sanhueza and Gabriel Canard

**Functionalized porphyrins from
meso-poly-halogeno-alkyl-dipyrromethanes: synthesis and
characterization**

MAPYRO: the French Fellowship of the Pyrrolic Macrocyclic Ring / *MAPYRO: la communauté française des macrocycles pyrroliques*

Functionalized porphyrins from *meso*-poly-halogeno-alkyl-dipyrromethanes: synthesis and characterization

Porphyrines fonctionnalisées au départ de meso-poly-halogéno-alkyle-dipyrrométhanes. Synthèse et caractérisation

Paul-Gabriel Julliard[®] *[a]*, **Simon Pascal**[®] *[a]*, **Olivier Siri**[®] *[a]*, **Diego Cortés-Arriagada**[®] *[b]*, **Luis Sanhueza**[®] *[, c, d]* **and Gabriel Canard**[®] *[, a]*

[a] Aix Marseille Univ, CNRS, CINaM, UMR 7325, Campus de Luminy, 13288 Marseille Cedex 09, France

[b] Programa Institucional de Fomento a la Investigación, Desarrollo e Innovación, Universidad Tecnológica Metropolitana, Ignacio Valdivieso 2409, San Joaquín, Santiago, Chile

[c] Departamento de Ciencias Biológicas y Químicas, Facultad de Recursos Naturales, Universidad Católica de Temuco, Temuco, Chile

[d] Núcleo de Investigatión en Bioproductos y Materiales Avanzados (BioMA), Universidad Católica de Temuco, Av. Rudecindo Ortega 02950, Temuco, Chile

E-mails: paul-gabriel.julliard@etu.univ-amu.fr (P.-G. Julliard), pascal@cinam.univ-mrs.fr (S. Pascal), olivier.siri@univ-amu.fr (O. Siri), dcortes@utem.cl (D. Cortés-Arriagada), luis.sanhueza@uct.cl (L. Sanhueza), gabriel.canard@univ-amu.fr (G. Canard)

Abstract. Starting from pyrrole-carbinol derivatives, a set of three optimized experimental conditions was used to prepare six dipyrromethanes (DPM) bearing *meso*-poly-halogeno-alkyl chains. On the one hand, the condensation of *p*-anisaldehyde and the DPMs bearing a perfluoroalkyl chain (CF_3, C_3F_7 or C_7F_{15}) produced, after oxidation, the expected *trans*-A_2B_2-porphyrins in reasonable yields. On the other hand, 5,15-diformyl-10,20-diarylporphyrin was directly obtained starting from the *meso*-(dichloromethyl)dipyrromethane, while traces of an unprecedented porphyrin bearing two *meso*-acyl fluoride groups were isolated from the use of the *meso*-(chlorodifluoromethyl)dipyrromethane. The straightforward formation of *bis*-formyl porphyrins is competitive compared to previously reported methods and has been extended to other benzaldehydes. The electron-withdrawing character of the

---

* Corresponding authors.

different substituents appended to porphyrins is enlightened through a combination of photophysical, electrochemical, structural and theoretical studies.

Résumé. En utilisant et en optimisant trois types de conditions expérimentales, six dipyrrométhanes (DPM) substitués en *meso* par des chaînes poly-halogénoalkyles ont été préparés. La condensation du *p*-anisaldéhyde sur les DPMs comportant des chaînes perfluoroalkyles (CF$_3$, C$_3$F$_7$ ou C$_7$F$_{15}$) produit, après oxydation, les porphyrines trans-A$_2$B$_2$ attendues avec des rendements corrects. En revanche, cette condensation conduit directement à des 5,15-diformyl-10,20-diaryl porphyrines au départ du *meso*-(dichlorométhyl)dipyrrométhane tandis que des traces d'une porphyrine originale comportant deux groupes fluorure d'acyle ont été isolées lorsque le *meso*-(difluoro-chlorométhyl)dipyrrométhane a été utilisé. La formation directe de *bis*-formyl porphyrines est compétitive et a été étendue à d'autres benzaldéhydes. Le caractère électro-attracteur des différents substituents introduits sur les porphyrines est mis en évidence par une combinaison d'études photophysiques, électrochimiques, structurales et théoriques.

Keywords. Dipyrromethanes, Porphyrins, Formylation, Acyl fluoride, Photophysics.

Mots-clés. Dipyrrométhanes, Porphyrines, Formylation, Fluorure d'acyle, Photophysique.

Available online 30th July 2021

1. Introduction

The synthesis and functionalization of porphyrinoid macrocycles are still the ongoing subjects of intense research activities because these exciting compounds are applied in numerous areas such as catalysis, biology or materials science [1–5]. One of the reasons for this major interest lies in the easy preparation of *meso*-substituted derivatives from the simple condensation of pyrrole and aldehydes which can produce, after oxidation and depending on the experimental conditions, a huge number of polypyrrolic and aromatic macrocycles such as porphyrins, corroles, contracted and expanded porphyrins [1–8]. The physico-chemical properties of these macrocycles can be tuned by the introduction of different *meso*-substituents that often require the prior synthesis of oligopyrrole precursors such as the widely used *meso*-substituted dipyrromethanes (DPMs). Though various synthetic procedures of *meso*-substituted-DPMs are described [9–12], very few are devoted to or can be applied to the preparation of derivatives bearing a *meso*-poly-halogenoalkyl group or a *meso*-perfluoroalkyl chain [13–23]. These specific substituents are however of major interest because, beyond their high electron-withdrawing character, they can confer to molecules a certain lipophilicity and/or an increased metabolic stability [24,25]. Moreover *meso*-perfluoroalkyl chains were shown to induce an important non-planar distortion [26–29] and a high photo-stability [30] when they occupy the *meso*-positions of porphyrins.

To the best of our knowledge, the DPMs **3a** and **3b** bearing respectively a *meso*-CF$_3$ group or a *meso*-C$_3$F$_7$ group are the only DPMs substituted by a *meso*-perfluoroalkyl chain for which synthetic procedures are described (Scheme 1). The common preparation of *meso*-substituted DPMs relies on the acid-catalyzed condensation of an aldehyde and pyrrole [9–12]. In boiling tetrahydrofuran (THF) and concentrated aqueous HCl (Scheme 1, route a), the condensation of stoichiometric amounts of pyrrole **1** and aldehydes **2a** or **2b** (as hemiacetal or as hydrate) gave for the first time the *meso*-perfluoroalkyl DPMs **3a** and **3b** with high yields (50–70% for **3a** and 35–50% for **3b**) [13]. Similar yields of **3b** were obtained by repeating this procedure [14–17] or by replacing the acid and the refluxing solvent by *p*-toluene sulfonic acid (PTSA) and CHCl$_3$, respectively (Scheme 1, route b) [18]. It was later shown that milder experimental conditions (Scheme 1, route c) also give high yields of **3a** (20–40%) and **3b** (35%) [19,20]. An original preparation of **3a** was reported by Dmowski *et al.* who used the sodium dithionite coupling of 1-bromo-1-chloro-2,2,2-trifluoroethane with **1** (Scheme 1, route d) [21,22].

If this simple and inexpensive procedure gives high yields of **3a** (49–58%), it can only be applied to incorporate this specific *meso*-substituent.

A key intermediate during the aldehyde-pyrrole condensation is the pyrrole-carbinol derivative **4** (Scheme 1). Such an intermediate bearing a heptafluoropropyl chain was prepared and dissolved with an excess of pyrrole in refluxing benzene containing PTSA (Scheme 1, route e) [23]. This stepwise strategy
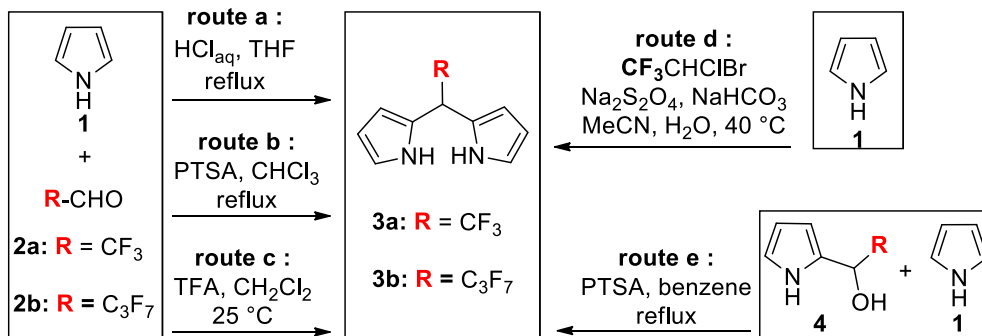
Scheme 1. Previous preparations of *meso*-perfluoroalkyl DPMs **3a** and **3b** (PTSA: *p*-toluene sulfonic acid).

produced **3b** with a high yield (77%). Having in mind that several 2-(polyhalogeno)acyl-pyrroles are easily prepared (or commercially available) and knowing that they are quantitatively reduced into the corresponding pyrrole-carbinol derivatives, we report herein how this latter strategy can be adapted, leading to a variety of *meso*-polyhalogenoalkyl DPMs. For this purpose, a set of three experimental conditions was selected and/or optimized to prepare the known **3a** and **3b** but also the unprecedented DPMs **3c–f** bearing on the *meso* position a perfluoroheptyl (**3c**), a chlorodifluoromethyl (**3d**), a dichloromethyl (**3e**) or a trichloromethyl group (**3f**).

These DPMs were involved in the synthesis of *trans*-A$_2$B$_2$-*meso*-substituted porphyrins through their acid-catalyzed condensation with *p*-anisaldehyde. The DPMs **3a–c** gave the expected porphyrins **6a–c** whereas the condensation of DPMs **3d** and **3e** led surprisingly to porphyrins bearing two *meso*-fluoroacyl groups (**6d**) and two *meso*-formyl groups (**6e**), respectively (Table 2). Other benzaldehydes were used to illustrate the straightforward access to 5,10-*bis*-(formyl)-15,20-diarylporphyrin because it is really competitive compared to previously described ones that were based on multistep elegant strategies such as: (a) the Vilsmeier formylation of copper porphyrins and their subsequent demetallations [31]; (b) the palladium catalyzed formation of *meso-bis*-(trimethyl)silylmethylporphyrins followed by their oxidation [32]; (c) the preparations and/or derivations of protected formyl groups (dithiane or acetal moieties) before the DPM-aldehyde condensation and their deprotections after the porphyrin ring formation [33,34].
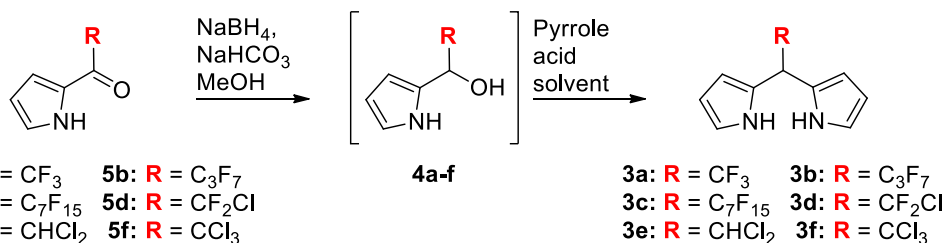
Because the physico-chemical properties of *meso*-perfluoro alkyl and *meso*-formyl porphyrins have been rarely described, those of the eight new free base porphyrins **6a–e**, **7**, **8** and **9** will be investigated in this contribution by a combination of photophysical, electrochemical and theoretical studies.

2. Results and discussion

2.1. *Synthesis*

The reaction of a slight excess of acyl-chloride or acid anhydride and pyrrole gave the 2-acyl pyrroles **5a–f** according to previously reported procedures (Table 1) [27,31]. These compounds were at first reduced to the corresponding carbinol derivatives **4a–f** using a slight excess of NaBH$_4$ (2 equiv.) in MeOH containing 2 equivalents of NaHCO$_3$ [35]. Because TLC analyses showed a complete conversion of the acylpyrroles **5a–f** and the formation of the alcohols **4a–f** with no observable side products, the pyrrole-carbinols **4a–f** were not isolated (nor characterized) but were always freshly prepared and used directly in the next condensation step (Table 1).

In 2011, a pyrrole-carbinol derivative analogous to **4a** but bearing an aryl group on the second α-position was condensated with pyrrole (2 equiv.) in dichloromethane (DCM) during 16 h at room temperature and using P$_2$O$_5$ (1 equiv.) as the activating agent [35]. These conditions gave very high yields of an asymmetrical *meso*-CF$_3$ DPM. Consequently, they were applied, in the present study, at the millimolar scale (condensation at 0.07 M in DCM) and using pyrrole **5a** to give **3a** with a yield of 60% (Table 1, entry 1).

Table 1. Optimization of the synthesis of DPMs **3a–f**

5a: **R** = CF$_3$ **5b:** **R** = C$_3$F$_7$
5c: **R** = C$_7$F$_{15}$ **5d:** **R** = CF$_2$Cl
5e: **R** = CHCl$_2$ **5f:** **R** = CCl$_3$

4a-f

3a: **R** = CF$_3$ **3b:** **R** = C$_3$F$_7$
3c: **R** = C$_7$F$_{15}$ **3d:** **R** = CF$_2$Cl
3e: **R** = CHCl$_2$ **3f:** **R** = CCl$_3$

Entry	Procedure	Reactant	R	[4a–f] (M)	Solvent[a]	Acid	Pyrrole/4a–f/acid	t (h)	Product	Yield (%)
1	**A**	**4a**	**CF$_3$**	**0.07**	**DCM**	**P$_2$O$_5$**	**2:1:2**	**16**	**3a**	**60**
2		4a	CF$_3$	0.23	DCM	P$_2$O$_5$	2:1:2	16	3a	39
3		4a	CF$_3$	7.28	—	P$_2$O$_5$	2:1:2	16	3a	44
4		4a	CF$_3$	0.58	Pyrrole	P$_2$O$_5$	25:1:2	16	3a	0
5		4a	CF$_3$	3.64	Pyrrole	Eaton's reagent[f]	4:1:1	1	3a	0[b]
6		4a	CF$_3$	0.2	THF[c]	HCl$_{aq}$	2:1:1.5	2	3a	26
7		4a	CF$_3$	0.15[d]	H$_2$O	HCl$_{aq}$	2:1:1.2	4	3a	22
8	**B**	**4a**	**CF$_3$**	**0.15[d]**	**H$_2$O**	**HCl$_{aq}$**	**2:1:1.2**	**16**	**3a**	**24 (28)[e]**
9		4a	CF$_3$	0.15[d]	H$_2$O	HCl$_{aq}$	2:1:1.2	40	3a	35
10		4a	CF$_3$	0.15[d]	H$_2$O	HCl$_{aq}$	4:1:1.2	16	3a	20
11	**A**	**4b**	**C$_3$F$_7$**	**0.07**	**DCM**	**P$_2$O$_5$**	**2:1:2**	**16**	**3b**	**52 (41)[e]**
12	B	4b	C$_3$F$_7$	0.15[d]	H$_2$O	HCl$_{aq}$	2:1:1.2	16	3b	0
13	**A**	**4c**	**C$_7$F$_{15}$**	**0.07**	**DCM**	**P$_2$O$_5$**	**2:1:2**	**16**	**3c**	**65 (87)[e]**
14	B	4c	C$_7$F$_{15}$	0.15[d]	H$_2$O	HCl$_{aq}$	2:1:1.2	16	3c	0
15	A	4d	CF$_2$Cl	0.07	DCM	P$_2$O$_5$	2:1:2	16	3d	0–2
16	**B**	**4d**	**CF$_2$Cl**	**0.15[d]**	**H$_2$O**	**HCl$_{aq}$**	**2:1:1.2**	**16**	**3d**	**18 (18)[e]**
17	**B**	**4e**	**CHCl$_2$**	**0.15[d]**	**H$_2$O**	**HCl$_{aq}$**	**2:1:1.2**	**16**	**3e**	**60 (67)[e]**
18	A	4f	CCl$_3$	0.07	DCM	P$_2$O$_5$	2:1:2	16	3f	0
19	B	4f	CCl$_3$	0.15[d]	H$_2$O	HCl$_{aq}$	2:1:1.2	16	3f	0
20		4f	CCl$_3$	0.2	DCM	TFA	1:1:1.2	16	3f	0
21		4f	CCl$_3$	0.2	THF[c]	HCl$_{aq}$	1:1:1.2	2	3f	3
22	**C**	**4f**	**CCl$_3$**	**0.2**	**THF[c]**	**HCl[g]**	**11:1:0.9**	**2**	**3f**	**9**

[a]All reactions were performed at room temperature unless otherwise noted. [b]Pyrrole polymerization occurs. [c]Reactions at reflux. [d]Resulting concentrations if pyrrole carbinol **4** was soluble in water. [e]Gram-scale yields are noted in brackets. [f]Eaton's reagent: P$_2$O$_5$ (7.7 wt%) in CF$_3$SO$_3$H. [g]HCl in Et$_2$O (1 M).

Higher concentrations or using pyrrole as the solvent did not improve the reaction yield (Table 1, entries 2–5). This procedure (Table 1, procedure A) was extended to pyrroles **5b,c** and afforded high amounts of **3b** (52%) and **3c** (65%) but only traces of **3d** (0–2%) and no **3f** (Table 1, entries 11, 13, 15 and 18). The preparation of **3b** and **3c** were repeated on a gram scale and gave DPMs with high yields.

To ensure better yields of **3d**, new experimental conditions were applied in the preparation of **3a**

from **4a** (used as a model compound). The utilization of refluxing THF and concentrated aqueous HCl was moderately efficient (Table 1, entry 6) but proved that the presence of water in the solvent was not detrimental to get *meso*-polyhalogeno alkyl DPMs. Several works have shown that *meso*-aryl-oligopyrrole syntheses can be performed in water and using concentrated aqueous HCl as catalyst [36–38]. The application of the conditions of Dehaen *et al.* [39] ([HCl] = 0.18 M, [**4a**] = 0.15 M, 2

equiv. of pyrrole, room temperature, 4 h) afforded **3a** with a yield of 22% that increases with the reaction time whereas higher amounts of pyrrole do not have any beneficial effect (Table 1, entries 7–10). We selected a reaction time of around one night (16 h) and applied these conditions (procedure B) to get DPMs **3b–f** (Table 1, entries 12, 14, 16 and 19). This procedure failed to give DPMs **3b,c** and **3f**, but produced **3d** and **3e** with up-scalable yields of 18% and 66% respectively.

Since mild conditions did not afford the DPM **3f**, and because the only example of a β-substituted DPM bearing a *meso*-CCl$_3$ group was obtained through harsh conditions (TFA as solvent, 40 °C) [40], we used again refluxing THF and HCl$_{(aq)}$ during the condensation step (Table 1, entry 21). A low yield of **3f** was obtained (3%) but reached 9% when using the experimental conditions described to synthesize a *meso*-CF$_3$ tripyrromethane from a DPM-mono-carbinol (Table 1, entry 22) [41]. Because no porphyrin could be, up to now, obtained from this particular DPM (*vide infra*), we have not pursued this optimization.
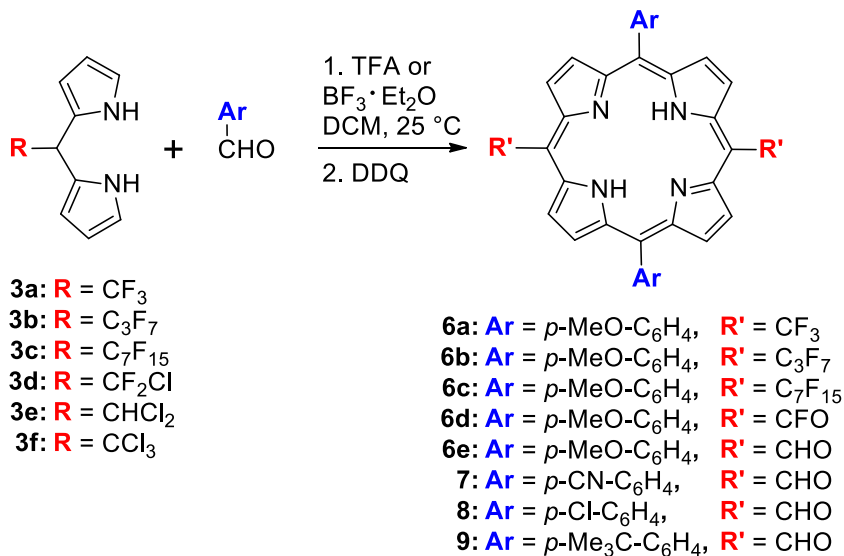
The DPMs **3a–f** were used as building blocks in the synthesis of porphyrins (Table 2). For this purpose, we chose to apply the conditions of the acid-catalyzed condensation of the DPMs **3a,b** with various aromatic aldehydes that were shown to be effective in the preparation of *trans*-A$_2$B$_2$ porphyrins bearing two *meso*-perfluoroalkyl groups (Table 2) [19]. The reaction of *p*-anisaldehyde (0.01 M) with DPMs **3a–f** catalyzed by TFA (10 equiv.) or by BF$_3$·OEt$_2$ (0.33 equiv.) in DCM was stopped after the complete disappearance of the DPMs (TLC analysis). The two catalysts have been tested and this contribution reports only the conditions giving the highest yields.

After oxidation by DDQ (1.5 equiv.) and purification by chromatography, modest yields (4–9%) of the *trans*-A$_2$B$_2$ porphyrins **6a–c** were obtained from the DPMs **3a–c** although, as previously described, no scrambling occurred during the condensation step [19].[1] It has to be noted that, in addition to the expected porphyrin, each experiment led to the formation of several other colored chromophores but

in too low yields to ensure their characterization. On the one hand, no porphyrin was detected from the reactions involving the DPM **3f** bearing a sterically hindered trichloromethyl group, while on the other hand, the less chlorinated DPMs **3d** and **3e** gave quite unexpected results (Table 2).

Unlike the common purple spots on TLC and purple solutions observed during the purification of porphyrin **3a–c**, green colored TLC spots and solutions were obtained while running the chromatography on the crude mixture from **3e**. The red-shifted UV–visible absorption of the isolated compound combined with its ^{1}H NMR spectrum featuring a downfield singlet located at 12.54 ppm were the first evidence of the exclusive formation of the *bis*-formyl porphyrin **6e** which was further confirmed by its HRMS analysis and its IR spectrum displaying an intense carbonyl stretching band at 1672 cm^{-1} (see the Supporting Information). The hydrolysis of the two CHCl$_2$ groups remains unexplained because it was neither observed during the preparation of DPM **3e** though being performed in acidic water, nor during its purification, which was also performed on silica gel. Suspecting that this hydrolysis would not have been quantitative, we performed another synthesis of **6e** and washed the reaction mixture with water after the oxidation step. This supplementary treatment led to an identical yield of **6e**. The CHCl$_2$ groups of the intermediate porphyrinogen have probably stability close to the CHCl$_2$ group of DPM **3e**. Their hydrolysis could occur during the oxidation step as it was previously observed after the condensation of a *meso*-nitromethyl DPM with an aromatic aldehyde leading to *meso*-formyl porphyrins [42]. Such hydrolysis was also observed during the metal-assisted cyclization of a *meso*-CHCl$_2$-β-substituted-*a,c*-biladiene into *meso*-formyl metallocorroles [43]. Because the simple use of DPM **3e** gives straightforward access to *trans*-*meso*-bis(formyl) porphyrin, it was extended to *p*-cyano-, *p*-chloro and *p*-*tert*-butyl-benzaldehydes and led in the same way to porphyrins **7**, **8** and **9** with respective yields of 9%, 2% and 12% (Table 2). The low isolated yield of **8** comes partly from its delicate purification due to its very low solubility in common organic solvents. In the same way, pure and solid **7** has only a slightly higher solubility. Consequently, a protonation–deprotonation sequence was used to ensure the complete dissolution of **7**, **8** and **9** when

---

[1] No other porphyrin was detected by TLC or during the chromatographic purification.

Table 2. Syntheses of porphyrins **6a–e**, **7**, **8** and **9**

3a: **R** = CF$_3$
3b: **R** = C$_3$F$_7$
3c: **R** = C$_7$F$_{15}$
3d: **R** = CF$_2$Cl
3e: **R** = CHCl$_2$
3f: **R** = CCl$_3$

6a: **Ar** = *p*-MeO-C$_6$H$_4$,   **R'** = CF$_3$
6b: **Ar** = *p*-MeO-C$_6$H$_4$,   **R'** = C$_3$F$_7$
6c: **Ar** = *p*-MeO-C$_6$H$_4$,   **R'** = C$_7$F$_{15}$
6d: **Ar** = *p*-MeO-C$_6$H$_4$,   **R'** = CFO
6e: **Ar** = *p*-MeO-C$_6$H$_4$,   **R'** = CHO
 7: **Ar** = *p*-CN-C$_6$H$_4$,   **R'** = CHO
 8: **Ar** = *p*-Cl-C$_6$H$_4$,   **R'** = CHO
 9: **Ar** = *p*-Me$_3$C-C$_6$H$_4$, **R'** = CHO

DPM	R	Acid	Porphyrin	Ar	R$'$	Yield (%)
3a	CF$_3$	BF$_3$	**6a**	*p*-MeO–C$_6$H$_4$–	CF$_3$	9
3b	C$_3$F$_7$	TFA	**6b**	*p*-MeO–C$_6$H$_4$–	C$_3$F$_7$	4
3c	C$_7$F$_{15}$	TFA	**6c**	*p*-MeO–C$_6$H$_4$–	C$_7$F$_{15}$	4
3d	CFCl$_2$	BF$_3$	**6d**	*p*-MeO–C$_6$H$_4$–	CFO	2
3e	CHCl$_2$	TFA	**6e**	*p*-MeO–C$_6$H$_4$–	CHO	11
3e	CHCl$_2$	TFA	**7**	*p*-CN–C$_6$H$_4$–	CHO	9
3e	CHCl$_2$	TFA	**8**	*p*-Cl–C$_6$H$_4$–	CHO	2
3e	CHCl$_2$	TFA	**9**	*p*-Me$_3$C–C$_6$H$_4$–	CHO	12

R$'$ groups are at the 5,15 positions, **Ar** are at the 10,20 positions.

recording their physico-chemical properties (see the experimental part).

As observed during the porphyrin synthesis starting from DPM **3e**, the acid-catalyzed condensation of DPM **3d** with *p*-anisaldehyde gave, after oxidation, a green spot on TLC and a green solution during the purification on silica. After purification, the red-shifted UV–visible spectrum of the isolated porphyrin **6d** together with the presence of a single signal at −62.63 ppm in its ^{19}F NMR spectrum indicated that the former CF$_2$Cl group borne by DPM **3d** had probably disappeared in **6d**. The unexpected structure of the *bis*-fluoro-acyl derivative **6d** was elucidated thanks to its HRMS analysis and its IR spectrum featuring a carbonyl stretching band at 1796 cm^{-1} (see the Supporting Information). Although the yield of this transformation is low (≤2%), it gave repeatedly

the first example of a porphyrin-bearing *meso*-fluoro acyl groups. As for **6e**, we are not able yet to give the causes and/or the mechanism of the peculiar hydrolysis that has been rarely observed [44] although it has been reported that C–X bonds of *meso*-perfluoroalkyl groups borne by DPMs or porphyrins are prone to be involved in eliminations, intramolecular cyclization or solvolysis processes [45–50].

2.2. *Electrochemical analysis of porphyrins 6a–e and 9*

The cyclic voltammograms (CVs) of **6a–e** and **9** were recorded in DCM containing 0.1 M of [(*n*Bu$_4$N)PF$_6$] (Figure 1 and Figure S1 in the Supporting Information). The corresponding oxidation and reduction half-wave and peak potential values are listed

Table 3. Half-wave and peak potentials (V versus SCE) of porphyrins **6a–e**, **9**, **(CF$_3$)$_4$PH$_2$** and **(C$_3$F$_7$)$_4$PH$_2$** measured in CH$_2$Cl$_2$ containing 0.1 M of [(^{n}Bu$_4$N)PF$_6$] (scan rate of 100 mV/s)

	R10,20	R5,R15	Reduction		Oxidation		ΔE (V)[a]
			Second	First	First	Second	
6a	4-OCH$_3$–C$_6$H$_4$	CF$_3$	−1.33[b]	−0.81 (100)[c]	1.32[b]	1.79[b]	2.11
6b	4-OCH$_3$–C$_6$H$_4$	C$_3$F$_7$	−1.34[b,d]	−0.80 (80)[c]	1.31[b]	1.75[b]	2.09
6c	4-OCH$_3$–C$_6$H$_4$	C$_7$F$_{15}$		−0.81 (100)[c]	1.29[b]	1.78[b]	2.08
6d	4-OCH$_3$–C$_6$H$_4$	CFO	−0.79 (107)[c]	−0.54 (72)[c]	1.39[b]		1.93
6e	4-OCH$_3$–C$_6$H$_4$	CHO	−0.89 (74)[c]	−0.57 (64)[c]	1.33[b]	1.81[b]	1.90
9	4-Me$_3$C–C$_6$H$_4$	CHO	−0.90 (73)[c]	−0.58 (69)[c]	1.40[b]	—	1.98
10[d]	4-PO$_3$Et$_2$–C$_6$H$_4$[d]	C$_3$F$_7$		−0.81		1.43	2.24
(CF$_3$)$_4$PH$_2$[e]	CF$_3$	CF$_3$		−0.48[f] (160)[c]			
(C$_3$F$_7$)$_4$PH$_2$[e]	C$_3$F$_7$	C$_3$F$_7$		−0.44[f] (158)[c]			

[a]HOMO–LUMO electrochemical gap calculated by $\Delta E = E_{1/2}(\text{ox}_1) - E_{1/2}(\text{red}_1)$ or by $\Delta E = E_{\text{pa}}(\text{ox}_1) - E_{1/2}(\text{red}_1)$. [b]Irreversible peak potential at a scan rate of 100 mV/s. [c]$\Delta E_{\text{p}} = E_{\text{pa}} - E_{\text{pc}}$ in mV. [d]A third irreversible reduction peak is placed at $E_{\text{pc}} = -1.56$ V versus SCE. [d]From Ref. [17]. [e]From Ref. [51]. [f]Measured in benzonitrile.

in Table 3 together with those of the *tetra-meso*-CF$_3$ porphyrin **(CF$_3$)$_4$PH$_2$** [51], the *tetra-meso*-C$_3$F$_7$ porphyrin **(C$_3$F$_7$)$_4$PH$_2$** [51], and of the porphyrin **10** analogous to **6b** but where the *p*-anisyl groups are replaced by *p*-diethylphophonate-phenyl substituents [17]. Each CV features a first reversible reduction and a first irreversible oxidation centered on the porphyrin ring. For the perfluoro derivatives **6a–c**, this oxidation seemed to be reversible at a scan rate of 100 mV/s but proved to be irreversible when increasing the scan rate up to 800 mV/s. Depending on the substituents, a second oxidation and/or a second reduction were also enlightened by the CVs of **6a–e**.

No oxidation could be observed previously when recording the CVs of **(CF$_3$)$_4$PH$_2$** and **(C$_3$F$_7$)$_4$PH$_2$** (Table 3) [51]. The replacement of two of these chains by *p*-anisyl groups in **6a** and **6b** leads to a significant negative shift of the first reduction potential (∼300 mV) and allows access to the data corresponding to the macrocycle oxidation ($E_{1/2} \sim 1.3$ V versus SCE).

Whereas the electrochemical properties of porphyrins are substantially varying with the number of *meso*-perfluoroalkyl chain, they are not notably tuned by the length of these lipophilic chains because the first oxidation/reduction potential values of **6a**, **6b** and **6c** are nearly the same (Table 3). Interestingly, the comparison between **6b** and **10**
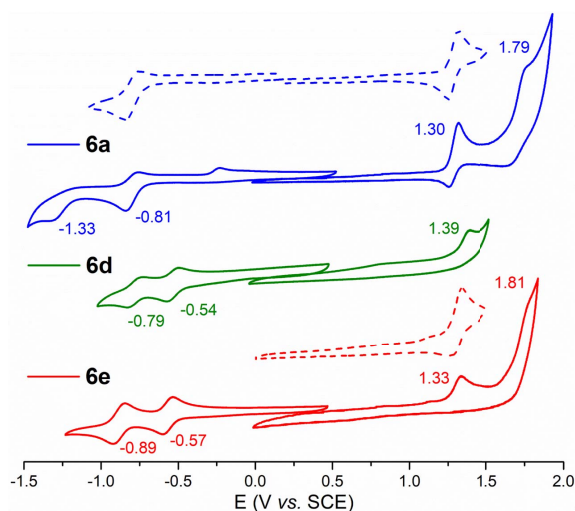
Figure 1. CVs of porphyrins **6a** (—), **6d** (—) and **6e** (—) in DCM containing 0.1 M of [(nBu$_4$N)PF$_6$] (scan rate of 100 mV·s^{-1}). The dotted traces emphasize the reversibility of selected redox processes.

shows that decreasing the electron richness of the 10,20-aryl groups shifts, as expected, the first oxidation process to higher potential values but leaves unchanged the energy of the first reduction. Therefore, varying the nature of 10,20-aryl groups has probably little influence on the energy of the LUMO of such

*trans*-A$_2$B$_2$ porphyrins which is controlled by the *meso*-perfluoroalkyl chains.

The important anodic shift (+240 mV) affecting the first reduction process when replacing CF$_3$ moieties in **6a** by formyl groups in **6e** cannot be explained by a field/inductive effect because the latter is stronger for CF$_3$ than for CHO (Hammett parameters: σ$_p$ (CF$_3$) = +0.54, σ$_p$ (CHO) = +0.42) [52]. A positive shift is also observed between the two corresponding macrocycle-centered oxidations but has a little amplitude (~30 mV) (Table 3). As for the CF$_3$ porphyrins **6b** and **10**, modifying the aryl groups in the formyl-substituted macrocycles **6e** and **9** produces only a slight modification of the first oxidation potential whereas the reduction potentials remain unchanged. It has to be noted that the solubility of **7** and **8** was too low in DCM to record accurate electrochemical data.

Supplementary anodic shifts are affecting the first reduction and potential processes when two CFO groups are appended by the porphyrin ring in **6d**. Therefore, the remarkable reduced HOMO–LUMO electrochemical gaps of **6d** and **6e** compared to those of derivatives **6a–c** result from a π-conjugation between the carbonyl groups and the aromatic porphyrin ring that are put into evidence by theoretical calculations.

2.3. *Spectral properties of the porphyrins*

The absorption and corrected emission spectra of porphyrins **6a–e**, **7**, **8** and **9** were recorded in DCM at room temperature and are shown in Figure 2 and Figure S2 in the Supporting Information. The molar absorption coefficients and absorption maxima of these seven novel compounds are gathered in Table 4 with their emission maxima (excitation at λ = 590 nm) and fluorescence quantum yields. In order to give structure–properties relationships, selected photophysical data of **10** [17], **(CF$_3$)$_4$PH$_2$** [53] and of **(C$_3$F$_7$)$_4$PH$_2$** [53] are also given in Table 4 together with those of the porphyrins **11** [19] and **12** [32] analogous to **6a** and **6e** but where the *p*-anisyl groups are replaced by simple phenyl substituents.

As reported for the *meso*-bis-CF$_3$ porphyrin **11** [19], porphyrins **6a–c** exhibit absorption spectra that are distinct from that of the well known *tetra*-phenylporphyrin (TPP). Compared to TPP, their Soret bands are blue-shifted and broadened
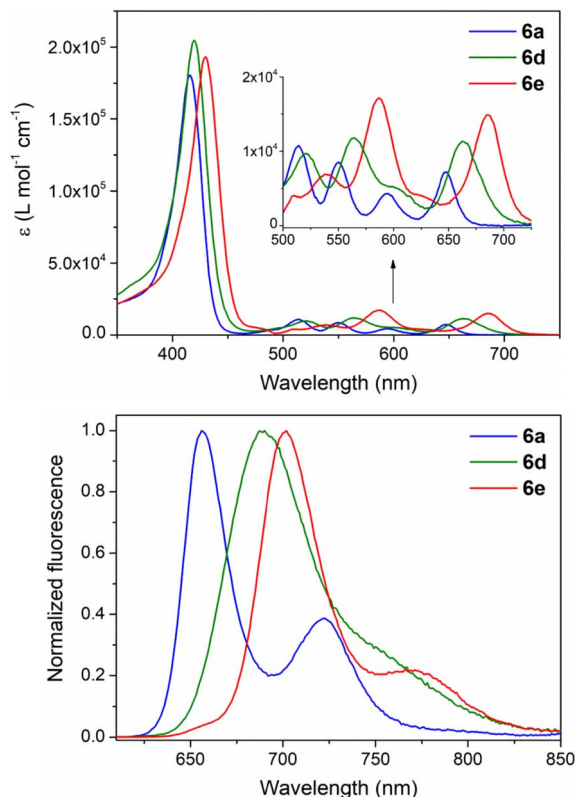
Figure 2. Electronic absorption spectra and normalized corrected emission spectra of porphyrins **6a** (—), **6d** (—) and **6e** (—) in aerated dichloromethane at room temperature.

(fwhm 27–28 nm) but significantly red-shifted compared to those of the *tetra*-perfluoroalkyl derivatives **(CF$_3$)$_4$PH$_2$** and **(C$_3$F$_7$)$_4$PH$_2$**.

In the same way, as shown for **11**, the Q bands of **6a–c** have absorption maxima close to those of TPP but with a different pattern. For example, the UV–visible spectra of the *trans*-A$_2$B$_2$ **6a–c** feature, as **10** and **11**, a noticeable increased intensity for the 0–0 component corresponding to a band at ca. 646 nm (Table 4). The length of the perfluoro alkyl chain has only a minor impact on the light-absorption and light-emission properties of **6a–c** that give similar fluorescence spectra and fluorescence quantum yields of ca. 7–9%. When comparing on the one hand the analogous **6a** and **11**, and on the other hand the analogous dyes **6b** and **10**, it can be noted that enhancing the electron richness of the aromatic

Table 4. UV–Vis and fluorescence data of porphyrins **6a–e**, **7**, **8**, **9–12**, **(CF₃)₄PH₂** and **(C₃F₇)₄PH₂** recorded in aerated dichloromethane at 298 K

			Absorption		Fluorescence	
	R10,20	R5,15	Soret band λ_{max} (nm) (ε (10^4 M^{-1}·cm^{-1}))	Q bands λ_{max} (nm) (ε (10^4 M^{-1}·cm^{-1}))	λ_{max}^{a} (nm)	Φ_{fl}^{b}
6a	4-OCH₃–C₆H₄	CF₃	416 (18.05) fwhm (28)[c]	514 (1.07), 550 (0.85), 595 (0.43), 648 (0.72)	658, 722	0.063
6b	4-OCH₃–C₆H₄	C₃F₇	414 (18.90) fwhm (28)[c]	514 (0.99), 551 (1.14), 595 (0.46), 646 (1.07)	656, 719	0.086
6c	4-OCH₃–C₆H₄	C₇F₁₅	415 (19.81) fwhm (27)[c]	514 (1.04), 552 (1.27), 596 (0.51), 647 (1.06)	655, 720	0.089
6d	4-OCH₃–C₆H₄	CFO	419 (20.46) fwhm (31)[c]	521 (0.97), 564 (1.18), 663 (1.13)	690	0.100
6e	4-OCH₃–C₆H₄	CHO	430 (19.32) fwhm (31)[c]	510 (0.40), 538 (0.69), 587 (1.71), 686 (1.49)	707, 771	0.079
7[d]	4-CN–C₆H₄	CHO	427 (10.30) fwhm (28)[c]	508 (0.23), 535 (0.38), 579 (0.85), 680 (0.75)	688, 757	0.057
8[d]	4-Cl–C₆H₄	CHO	427 (11.69) fwhm (30)[c]	535 (0.36), 583 (1.03), 682 (0.91)	692, 763	0.077
9[d]	4-Me₃C–C₆H₄	CHO	427 (20.64) fwhm (30)[c]	539 (0.62), 585 (1.75), 684 (1.54)	696, 767	0.081
10[e]	4-PO₃Et₂–C₆H₄	C₃F₇	410 (19.1)	510 (1.1), 546 (1.2), 590 (0.5), 643 (1.1)	647, 715	
11[f]	C₆H₅	CF₃	414 (16.50) fwhm (27)[c]	511 (1.01), 546 (1.01), 592 (0.53), 647 (0.77)	650, 720[f]	0.044
12[g]	C₆H₅	CHO	426 (15.85)	535 (0.50), 586 (1.26), 685 (1.00)		
(CF₃)₄PH₂[h]	CF₃	CF₃	408 (9.55)	512 (0.87), 546 (0.88), 596 (0.43), 651 (0.96)	654, 721	0.016
(C₃F₇)₄PH₂[h]	C₃F₇	C₃F₇	409 (9.23)	513 (0.92), 547 (0.75), 596 (0.43), 649 (0.97)	651, 718	0.021
TPP[i]	C₆H₅	C₆H₅	419 (47.00)	514 (1.87), 549 (0.77), 591 (0.54), 647 (0.34)	650, 715[j]	0.15[j]

[a] λ_{max} for the bands derived from corrected emission spectra. [b] Luminescence quantum yields in air-equilibrated dichloromethane by comparing corrected emission spectra and using tetraphenylporphyrin (TPP) in aerated acetonitrile as a standard (Φ_{fl} = 0.15 [54]). Excitation at λ = 590 nm. [c] Full width of half maximum in nm. [d] A protonation–deprotonation sequence was used to ensure a complete dissolution. [e] From Ref. [17], measured in CHCl₃/MeOH. [f] From Ref. [19], λ_{abs} and Φ_{fl} measured in toluene, λ_{em} measured in CH₂Cl₂/EtOH (3:1). [g] From Ref. [32], measured in CHCl₃. [h] From Ref. [53], measured in benzene. [i] From Ref. [19], measured in benzene. [j] Recorded in acetonitrile.

substituents induces a little red shift of the absorption and fluorescence maxima.

As observed when recording the electrochemical data, introducing *meso*-formyl groups produces a noticeable lower HOMO–LUMO optical gap. The UV–visible absorption and fluorescence bands of **6e** are importantly red-shifted. For example, the Soret band maximum of **6e** is at 430 nm and the 0–0 component of its Q bands can be found at 686 nm. Its quantum yield is as for **6a–c** of ca. 8%. Replacing electron-withdrawing aryl groups in **7** and **8** by electron-donating ones in **9** and **6e** produces a supplementary red shift of the absorption and emission bands.

For the unique **6d**-bearing *meso*-fluoro acyl moieties, it can be noted that its light-absorption and

emission bands are also red-shifted compared to those of **6a–c** and of TPP but with a lower amplitude. Its fluorescence spectrum has also a unique pattern with a single and broadened band at 690 nm corresponding to a quantum yield of 10%.

2.4. *Theoretical and structural studies of selected porphyrins*

DFT and Time-dependent DFT (TD-DFT) calculations were performed to analyze the effects of the *meso*-substituents CF₃, C₃F₇, C₇F₁₅, CFO and CHO on the structural, electronic and optical properties of porphyrins **6a–e**. The structures of **6a–e** were fully optimized and gave values of geometrical parameters

a)

b)

c)
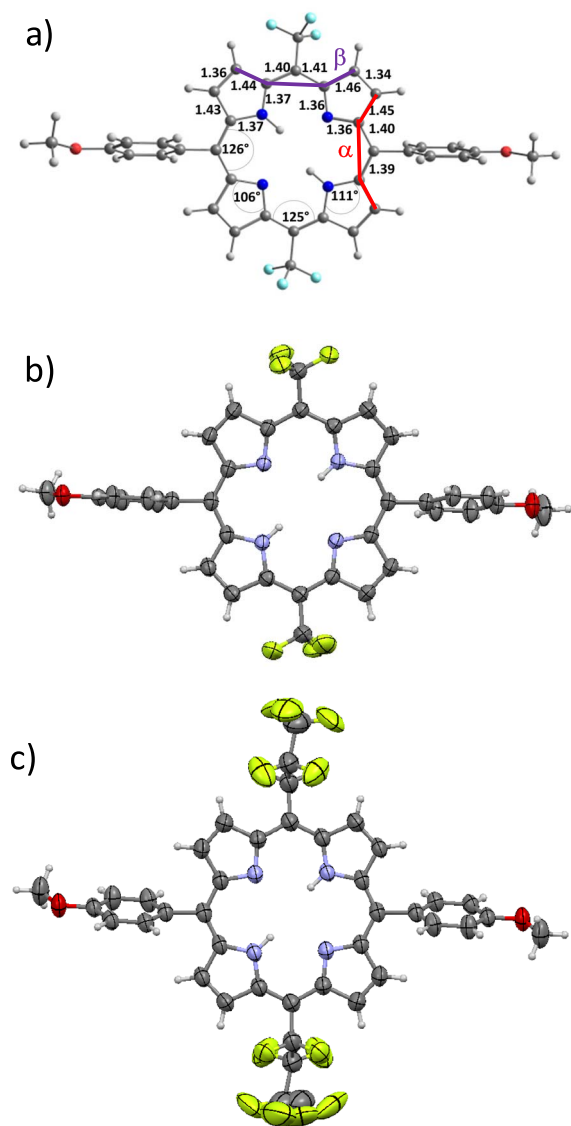
Figure 3. (a) Bond distances (Å), angle values (°) and external dihedral angles α and β of the optimized structure of **6a**; views of the single X-ray structures of (b) **6a** and (c) **6b** (solvent molecules are omitted for the sake of clarity).

such as bond distances, angles and dihedral angles that are illustrative of the effect of the *meso* substitutions on their core structures (Figure 3 and Figure S3 in the Supporting Information). Although there were no symmetry constraints in the calculation procedures, results did provide symmetric structures. Therefore, only parameters corresponding to

one-half of the porphyrin macrocycles are detailed in Figures 3 and S3. Very slight differences are observed between the bond distances and angle values of **6a–e** despite the variation of the nature of 5,15 *meso*-substituents (Figures 3 and S3). In fact, most relevant differences in the geometrical parameters are related to the values of the calculated external dihedral angles α and β which are listed in Table 5 and represented in Figure 3. These dihedral angles stand for the plane torsion regarding two adjacent pyrrole units of the porphyrin core center. As observed in Table 5, the α values are about 5.0° for **6a**-bearing CF_3 moieties and increase up to 10.6° for **6b** and **6c** substituted respectively by the more bulky C_3F_7 and C_7F_{15} substituents. The β values are quite low with values in the range of ~0.7°. On the other hand, the presence of CFO and CHO as highly acceptor moieties in **6d** and **6e** induces decreased α values of 7.8° and 7.2°, respectively, while significantly increased β values of 12.4° (**6d**) and 8.5° (**6e**) are observed for these systems. These results indicate that the introduction of CHO or CFO groups on the *meso*-positions produce a noticeable supplementary out-of-plane distortion of the macrocycles in **6d** and **6e** compared to those of the alkyl appended porphyrins **6a–c**.

During the final editing stages of this contribution, we were glad to get diffracting single crystals of porphyrins **6a** and **6b** (Figures 3(b) and (c)). As for the calculated geometries, the corresponding experimental structures feature a small out-of-plane distortion of the porphyrin **6a** and **6b** which is higher for **6b** and correspond to a slight ruffling of the macrocycles.

The frontier molecular orbitals (FMOs) of **6a–e** were also studied by DFT calculations. The energies of the two HOMOs and of the two LUMOs are listed in Table 5 and their plots are displayed in Figure 4 and Figure S4 in the Supporting Information. The calculated HOMO–LUMO gaps are in accordance with the experimental data and decrease in importance when fluoro acyl or formyl groups are borne by the 5 and 15 *meso*-positions. As observed during the UV–Vis absorption and electrochemical experiments, the lowest HOMO–LUMO gap is obtained for the bis-formyl derivative **6e**. For **6a–e**, the HOMO appears mainly to be located at the *p*-anisyl substituents, the core-*N* atoms and the *meso*-bridging carbon atoms at the 5,15 positions. Therefore, the lack of any apparent

Table 5. Calculated dihedral angles (°), experimental dihedral angles (°) and orbital energies (eV) of porphyrins **6a–e**

	R5,15	α (°)	β (°)	HOMO−1 (eV)	HOMO (eV)	LUMO (eV)	LUMO+1 (eV)
6a	CF$_3$	4.3 3.3[a]	0.7 6.4[a]	−5.36	−5.25	−3.47	−3.16
6b	C$_3$F$_7$	10.6 13.4[a]	0.7 6.5[a]	−5.37	−5.23	−3.49	−3.16
6c	C$_7$F$_{15}$	10.6	0.6	−5.38	−5.24	−3.50	−3.16
6d	CFO	7.8	12.4	−5.44	−5.27	−3.69	−3.23
6e	CHO	7.2	8.5	−5.40	−5.26	−3.78	−3.18

[a]Experimental dihedral angle values from the single crystal X-ray diffraction structures of **6a** and **6b**.
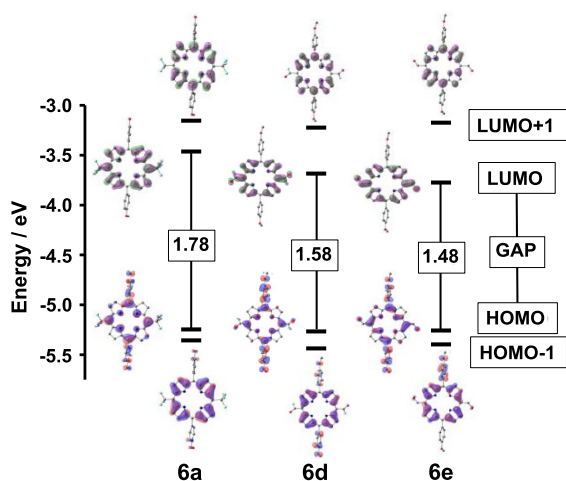
Figure 4. Plots of the calculated frontier orbitals and values of the HOMO–LUMO gaps (in eV) of **6a**, **6d** and **6e**.

contribution from the 5,15 substituents results in similar HOMO energy values differing by less than 1% for the **6a–e** series. Similarly, the five HOMO-1 and the five LUMO+1 of **6a–e** have energy values and electron density distributions that are only slightly varying with the nature of the 5,15 *meso*-substituents.

On the contrary, substantial differences appear when comparing the energies of the LUMOs. Those of **6a–c** have electron density distributions barely affected by the length of their perfluoroalkyl chains. Consequently, **6a**, **6b** and **6c** have quite identical FMOs energies and HOMO–LUMO gap values in accordance with the corresponding photophysical and electrochemical data. The LUMO iso-surfaces of **6d** and **6e** feature a remarkable participation of the π-conjugated *meso*-electron-withdrawing groups CFO

and CHO that are responsible for the concomitant lower LUMO energies and lower HOMO–LUMO gaps. The simulation of the UV–visible spectra of **6a–e** was obtained from further TD-DFT calculations and is detailed in the Supporting Information together with the corresponding compositions, vertical excitation energies, oscillator strengths and hole–electron excited states' surface distributions. For **6a–e**, theory gives Soret bands between 380 and 450 nm and these are red-shifted for **6d** and **6e** as observed experimentally. On the contrary, few differences are obtained when comparing the locations and intensities of the calculated Q bands of **6a–e**, because the different 5,15 *meso* substituents have only a slight impact on the corresponding electronic transitions.

3. Conclusions

Meso-polyhalogeno alkyl dipyrromethanes were prepared by the reduction of 2-acyl pyrroles and their subsequent acid-catalyzed reaction with pyrrole. Three sets of experimental conditions were optimized depending on the starting compound. This procedure lead firstly to the known DPMs **3a** and **3b** substituted by a trifluoromethyl group and a heptafluropropyl chain, respectively. New derivatives were also obtained, bearing on the *meso*-position a perfluoroheptyl (**3c**), a chlorodifluoromethyl (**3d**), a dichloromethyl (**3e**) or a trichloromethyl group (**3f**). Dipyrromethanes are useful compounds in the synthesis of various chromophores including BODIPYs, corroles or expanded porphyrins. Herein, they were used to build trans-A$_2$B$_2$ *meso*-substituted porphyrins through their condensation with aromatic aldehydes. The perfluoro DPMs produce the expected bis-alkylporphyrins while exciting *meso*-functionalized analogs were obtained from DPMs

3d and **3e**-bearing chlorine atoms. Indeed, several bis-formyl porphyrins were prepared directly from **3e** and illustrate an original and straightforward strategy to get such derivatives. Similarly, the use of **3d** leads to **6d** as a unique example of a porphyrin-bearing *meso*-fluoro acyl moieties. The electron-withdrawing character of the perfluoralkyl chains and of the π-conjugated formyl and fluoro acyl groups were investigated and enlightened thanks to photophysical and electrochemical analyses supported by theoretical calculations. These studies revealed, for example, that when appended by porphyrins, formyl and fluoro acyl functional groups give to the macrocycles reduced HOMO–LUMO electrochemical gaps and red-shifted absorption and emission properties.

4. Experimental section

4.1. *Materials*

All reagents were used as received. Pyrrole was distilled before use. The distillation of THF was performed on sodium/benzophenone. Flash column chromatography was performed on silica gel 60 (230–400 mesh). Visualization of DPM **3a–f** TLC spots was achieved by staining the TLC plates with a solution of phosphomolybdic acid (2.5 g) in ethanol and by subsequent heating.

4.2. *Physical measurements*

^{1}H, ^{13}C and ^{19}F nuclear magnetic resonance (NMR) spectra were recorded on a JEOL ECS400 NMR spectrometer at room temperature. NMR chemical shifts are given in ppm (δ) relative to Me$_4$Si using solvent residual peaks as internal standards (CDCl$_3$: δ = 7.26 ppm for ^{1}H and 77.2 for ^{13}C; Acetone-d_6: δ = 2.05 ppm for ^{1}H and 29.8 for ^{13}C; DMSO-d_6: δ = 2.50 ppm for ^{1}H and 39.5 for ^{13}C). IR spectra were recorded on an Agilent Cary 630 FTIR equipped with an attenuated total reflectance (ATR) sampling. Melting points (M.P.) were measured in open capillary tubes with a STUART SMP30 melting points apparatus and are uncorrected. High resolution mass spectrometry (HRMS-ESI) analyses were performed on a QStar Elite (Applied Biosystems SCIEX) spectrometer or on a SYNAPT G2 HDMS (Waters) spectrometer by the "Spectropole" of Aix-Marseille University.

These two instruments are equipped with an electrospray ionization (ESI) or a MALDI source and a TOF analyser.

4.3. *Electronic absorption and fluorescence*

UV–Vis absorption spectra were recorded in spectrophotometric grade solvents (ca. 10^{-6} M) on a Varian Cary 50 SCAN spectrophotometer. Ten equivalents of TFA were added to the suspension of the porphyrins **7**, **8** and **9** in order to ensure their complete dissolution as protonated and non-aggregated dyes. A subsequent addition of twelve equivalents of ^{i}Pr$_2$NEt afforded back the non-protonated free bases soluble in solution. Emission spectra were obtained using a Horiba-Jobin Yvon Fluorolog-3 spectrofluorimeter equipped with a three-slit double-grating excitation and a spectrograph emission monochromator with dispersions of 2.1 nm·mm^{-1} (1200 grooves per mm). A 450 W xenon continuous wave lamp provided excitation. Fluorescence of diluted solutions was detected at right angle using 10 mm quartz cuvettes. Fluorescence quantum yields Φ were measured in diluted dichloromethane solutions with an optical density lower than 0.1 using the following equation:

$$\frac{\Phi_x}{\Phi_r} = \left(\frac{A_r(\lambda)}{A_x(\lambda)}\right)\left(\frac{n_x^2}{n_r^2}\right)\left(\frac{D_x}{D_r}\right)$$

where A is the absorbance at the excitation wavelength (λ), n the refractive index and D the integrated intensity. "r" and "x" stand for reference and sample. The fluorescence quantum yields were measured relative to tetraphenylporphyrin (TPP) in acetonitrile (Φ = 0.15) [54]. Excitation of reference and sample compounds was performed at the same wavelength (590 nm).

4.4. *Electrochemistry*

Cyclic voltammetric (CV) data were acquired using a BAS 100 Potentiostat (Bioanalytical Systems) and a PC computer containing BAS100W software (v2.3). A three-electrode system with a Pt working electrode (diameter 1.6 mm), a Pt counter electrode and a leak-free Ag/AgCl reference electrode (diameter 5 mm) was used. [^{n}Bu$_4$N]PF$_6$ (0.1 M in CH$_2$Cl$_2$) served as an inert electrolyte while the concentration of the electro-active compound is of ca. 5×10^{-4} M.

Cyclic voltammograms were recorded at a scan rate of 100 mV·s⁻¹. Ferrocene (0.46 V/SCE) was used as internal standard [55]. Solutions were degassed using argon and the working electrode surface (Pt) was polished before each scan recording. The solubility of porphyrins **7** and **8** in the solvent is too low to get accurate electrochemical values.

4.5. *Computational details*

All (TD-)DFT calculations have been performed using the Gaussian 16 program [56]. The geometry optimizations were carried out without symmetry constraints to ensure the minima energy. Calculations were performed using the CAM-B3LYP exchange functional (since this level of theory have been widely used in this type of compounds and also because this functional reproduces correctly the corresponding geometrical parameters) and the 6-311+G(d,p) basis set for all atoms [57,58]. Frequency calculations were also included to corroborate the optimized structures, showing only positive values in all vibrational modes. TD-DFT calculations were performed for the first 80 vertical excitations, in vacuum and in dichloromethane (DCM) as solvent, using the conductor-like polarizable continuum model (CPCM) [59]. Here, the BLYP functional was implemented in conjunction with the 6-311+G(d,p) basis set for all atoms. The BLYP functional was chosen because this level of theory accurately reproduces the experimental UV–Vis results [60].

4.6. *Single crystal X-ray diffraction*

Suitable diffracting single crystals of **6a** and **6b** were obtained by slow diffusion of *n*-pentane into concentrated solutions of the porphyrins in dichloromethane. The intensity data for compound **11a** were collected on a Rigaku Oxford Diffraction SuperNova diffractometer using CuKα radiation (λ = 1.54184 Å) at 293 K. Data collection, cell refinement and data reduction were performed with CrysAlisPro (Rigaku Oxford diffraction). Using Olex2 [61], the structures were solved with shelXT [62] and shelXL [62] was used for full matrix least squares refinement. CCDC-2074306 (**6a**) and CCDC-2074307 (**6b**) contain the supplementary crystallographic data. These data can be obtained free of charge from The Cambridge Crystallographic Data Centre via www.ccdc.cam.ac.uk/data_request:cif.

4.7. *Synthetic methods*

The 2-acylpyrroles **5a** (R = CF₃) [63], **5b** (R = C₃F₇) [26], **5c** (R = C₇F₁₅) [64], **5f** (R = CCl₃) [65] and **5e** (R = CHCl₂) [66] were prepared as previously reported.

4.7.1. *2-(Chlorodifluoroacetyl)pyrrole (5d)*

This compound was prepared following a protocol adapted from the synthesis of 2-(trifluoroacetyl)-pyrrole **5a** [63]. A solution of chlorodifluoroacetic anhydride (4.15 mL, 23 mmol, 1.1 equiv.) in anhydrous CH₂Cl₂ (15 mL) was cooled to −15 °C under an argon atmosphere. A solution of pyrrole (1.44 mL, 20.9 mmol, 1 equiv.) in anhydrous CH₂Cl₂ (15 mL) was then added dropwise under firm stirring. The mixture was stirred at −15 °C for 1.5 h, then at room temperature during an additional hour. The organic phase was washed with water, dried over Na₂SO₄, and the solvent removed by evaporation. The resulting residue was purified by flash chromatography (CH₂Cl₂/petroleum ether 1:1) to afford **5d** as a white solid (4.01 g, 22 mmol, 99%).

R$_F$ = 0.45 (silica, CH₂Cl₂/petroleum ether 1:1). **Mp:** 41.9 °C; **¹H NMR (CDCl₃) δ** = 10.27 (br s, 1H, NH), 7.28 (m, 1H, α-H), 7.25 (m, 1H, β-H), 6.41 (m, 1H, β-H) ppm; **¹⁹F NMR (CDCl₃) δ** = −61.5 ppm; **¹³C {¹H} NMR (CDCl₃) δ** = 172.2 (t, ²$J_{C,F}$ = 30.5, C), 129.6 (CH), 124.7 (C), 122.1 (t, ⁴J_{C-F} = 4.7, CH), 120.5 (t, ¹$J_{C,F}$ = 302.5, C), 112.7 (CH) ppm; **IR: v͂** = 3329 (vs, N–H), 1638 (vs, C=O) cm⁻¹; **HMRS-ESI:** calcd. for C₆H₃NOF₂Cl [M–H]⁻ 177.9877. Found: 177.9877.

4.7.2. *5-(Trifluoromethyl)dipyrromethane (3a)*

Procedure A: to a solution of 2-(trifluoroacetyl)-pyrrole **5a** (500 mg, 3.07 mmol, 1 equiv.) and NaHCO₃ (514 mg, 6.13 mmol, 2 equiv.) suspended in methanol (46 mL) under firm stirring was added NaBH₄ (232 mg, 6.12 mmol, 2 equiv.) by portions. The mixture was stirred at room temperature for 30 min before removal of the solvent by evaporation. The crude product was dissolved in Et₂O. This organic phase was washed with water, dried over Na₂SO₄ and evaporated at 30 °C. The resulting residue and pyrrole (0.42 mL, 6.12 mmol, 2 equiv.) were dissolved in CH₂Cl₂ (40 mL) and under argon atmosphere. P₂O₅ (87 mg, 6.13 mmol, 2 equiv.) was then added and the mixture was stirred at room temperature for 16 h. A saturated aqueous NaHCO₃ solution (10 mL) was added, and the stirring maintained for 1 h. The

crude product was filtered and washed with DCM on a Büchner funnel equipped with sintered glass. The filtrate was dried on Na_2SO_4. The subsequent flash chromatography (CH_2Cl_2/petroleum ether 1:1, then 2:1) afforded **3a** as a white solid (395 mg, 1.8 mmol, 60%).

Procedure B: to a solution of 2-(trifluororoacetyl)-pyrrole **5a** (250 mg, 1.53 mmol, 1 equiv.) and $NaHCO_3$ (257 mg, 3.06 mmol, 2 equiv.) suspended in methanol (4.6 mL) under firm stirring was added $NaBH_4$ (116 mg, 3.06 mmol, 2 equiv.) by portions. The mixture was stirred at room temperature for 30 min before removal of the solvent by evaporation. The crude product was extracted with Et_2O, then washed with water and dried over Na_2SO_4. The organic phase was evaporated at 30 °C then dissolved with pyrrole (0.21 mL, 3.06 mmol, 2 equiv.), in an aqueous HCl solution (0.18 M, 5 mL). The mixture was stirred at room temperature for 16 h. The mixture was then extracted with CH_2Cl_2. This organic phase was washed with water, dried on Na_2SO_4 before removal of the solvent by evaporation. The residue was finally purified by flash chromatography (CH_2Cl_2/petroleum ether 2:1) to afford **3a** as a gray solid (79 mg, 0.37 mmol, 24%). **Scale up:** starting from 2-(trifluororoacetyl)pyrrole **5a** (2.5 g, 15.3 mmol, 1 equiv.), **3a** was obtained as a gray solid (938 mg, 4.4 mmol, 28%).

R_F = 0.5 (CH_2Cl_2/petroleum ether 2:1). **^{1}H NMR (CDCl$_3$) δ** = 8.10 (br s, 2H, NH), 6.77 (m, 2H, α-H), 6.25 (m, 2H, β-H), 6.22 (m, 2H, β-H), 4.85 (q, $^3J_{H,F}$ = 9.0, 1H, *meso*-H) ppm; **IR: v~** = 3366, 3346 (vs, N–H), 1242, 1161, 1119, 1092, 1043 (s, C–F) cm^{-1}. Other analytical data are consistent with literature values [13].

4.7.3. *5-(Perfluoropropyl)dipyrromethane (3b)*

Procedure A: scale up: to a solution of 2-(perfluorobutyryl)pyrrole **5b** (4.18 g, 15.9 mmol, 1 equiv.) and $NaHCO_3$ (2.67 g, 31.8 mmol, 2 equiv.) suspended in methanol (50 mL) under firm stirring was added $NaBH_4$ (1.20 g, 31.8 mmol, 2 equiv.) by portions. The mixture was stirred at room temperature for 30 min before removal of the solvent by evaporation. The crude product was dissolved in Et_2O. The organic phase was washed with water, dried over Na_2SO_4 and was evaporated at 30 °C. The resulting residue and pyrrole (2.21 mL, 31.8 mmol, 2 equiv.) were dissolved in CH_2Cl_2 (200 mL) under argon. P_2O_5 (4.51 g, 31.8 mmol, 1 equiv.) was then added

and the mixture was stirred at room temperature for 16 h. $NaHCO_3$ (3.47 g, 41.3 mmol, 2.6 equiv.) was added and the stirring maintained for 1 h. The mixture was filtrated and washed with DCM on a Büchner funnel equipped with sintered glass. The filtrate was dried on Na_2SO_4 before removal of the solvent by evaporation. The residue was finally purified by flash chromatography (CH_2Cl_2/petroleum ether 2:1) to afford **3b** as a white solid (2.05 g, 6.5 mmol, 41%).

R_F = 0.65 (silica, CH_2Cl_2/petroleum ether 2:1). **^{1}H NMR (CDCl$_3$) δ** = 8.15 (br s, 2H, NH), 6.78 (m, 2H, α-H), 6.25 (m, 2H, β-H), 6.20 (m, 2H, β-H), 4.94 (t, $^3J_{H,F}$ = 16.6, 1H, *meso*-H) ppm; **IR: v~** = 3368 (s, N–H), 1233, 1207, 1175, 1113, 1093 (s, C–F) cm^{-1}. Other analytical data are consistent with literature values [13].

4.7.4. *5-(Perfluoroheptyl)dipyrromethane (3c)*

Procedure A: scale up: to a solution of 2-(perfluoro-octanoyl)pyrrole **5c** (2.01 g, 4.31 mmol, 1 equiv.) and $NaHCO_3$ (722 mg, 8.60 mmol, 2 equiv.) suspended in methanol (16 mL) under firm stirring was added $NaBH_4$ (325 mg, 8.59 mmol, 2 equiv.) by portions. The mixture was stirred at room temperature for 30 min before removal of the solvent by evaporation. The crude product was dissolved in Et_2O. The organic phase was washed with water, dried over Na_2SO_4 and was evaporated at 30 °C. The resulting residue and pyrrole (0.6 mL, 8.62 mmol, 2 equiv.) were dissolved in CH_2Cl_2 (65 mL) under argon. P_2O_5 (1.22 g, 8.65 mmol, 2 equiv.) was then added and the mixture was stirred at room temperature for 16 h. $NaHCO_3$ (940 mg, 11.2 mmol, 2.6 equiv.) was added and the stirring maintained for 1 h. The crude product was filtrated and washed by DCM on a Büchner funnel equipped with sintered glass. The filtrate was dried on Na_2SO_4 before removal of the solvent by evaporation. The residue was finally purified by flash chromatography (CH_2Cl_2/petroleum ether) to afford **3c** as a light purple solid (1.92 g, 3.73 mmol, 87%).

R_F = 0.60 (silica, CH_2Cl_2/petroleum ether). **^{1}H NMR (CDCl$_3$) δ** = 8.15 (br s, 2H, NH), 6.78 (m, 2H, α-H), 6.25 (m, H, β-H), 6.20 (m, 2H, β-H), 4.96 (t, $^3J_{H,F}$ = 16.8, 2H, *meso*-H) ppm; **^{19}F NMR (CDCl$_3$) δ** = −80.7 (CF$_3$), −112.2, −120.5, −121.5, −121.9, −122.6, −126.0 ppm; **^{13}C {^{1}H} NMR (CDCl$_3$) δ** = 122.3 (C), 119.0 (CH), 109.7 (CH), 109.1 (CH), 108.3 (C), 41.2 (t, $^2J_{C-F}$ = 23.0, C) ppm, other carbon atoms could not be assigned due the low intensity of the

perfluorinated chain peaks [67] and because of the rapid degradation of the compound in solution; **IR: $\tilde{v}$** = 3405 (br, N–H), 1235, 1198, 1143, 1095 (vs, C–F) cm^{-1}; **HRMS-ESI:** calcd for $C_{16}H_8F_{15}N_2$ [M–H]$^-$: 513.0453. Found: 513.0461.

4.7.5. *5-(Chlorodifluoromethyl)dipyrromethane (3d)*

Procedure B: to a solution of 2-(chlorodifluoroacetyl)pyrrole **5d** (100 mg, 0.56 mmol, 1 equiv.) and NaHCO$_3$ (94 mg, 1.12 mmol, 2 equiv.) suspended in methanol (1.7 mL) under firm stirring was added NaBH$_4$ (42 mg, 1.1 mmol, 2 equiv.) by portions. The mixture was stirred at room temperature for 30 min before removal of the solvent by evaporation. The crude product was dissolved with Et$_2$O. This organic phase was washed with water, dried over Na$_2$SO$_4$ and evaporated at 30 °C. The resulting residue was then dissolved in pyrrole (0.78 mL, 1.1 mmol, 2 equiv.) before the addition of an aqueous HCl solution (0.18 M, 2 mL). The mixture was stirred at room temperature for 16 h. The mixture was then extracted with CH$_2$Cl$_2$, washed with water, and dried on Na$_2$SO$_4$ before removal of the solvent by evaporation. The subsequent flash chromatography (CH$_2$Cl$_2$/petroleum ether 2:1) afforded **3d** as a white solid (23 mg, 0.1 mmol, 18%). **Scale up:** The same procedure at a larger scale and starting from **5d** (2.74 g, 15.3 mmol) afforded **3d** as a white solid (589 mg, 2.55 mmol, 18%).

R$_F$ = 0.65 (silica, CH$_2$Cl$_2$/petroleum ether 2:1). **Mp:** 75–80 °C; **^{1}H NMR (CDCl$_3$) δ** = 8.19 (br s, 2H, NH), 6.79 (m, 2H, α-H), 6.27 (m, 2H, β-H), 6.22 (m, 2H, β-H), 4.96 (t, $^3J_{H,F}$ = 11.1, 1H, *meso*-H) ppm; **^{19}F NMR (CDCl$_3$) δ** = −53.3 (d, $^3J_{F,H}$ = 11.1) ppm; **^{13}C {^{1}H} NMR (CDCl$_3$) δ** = 118.7 (CH), 117.8 (C), 109.6 (t, $^2J_{C,F}$ = 1.4, CH), 109.1 (CH), 108.3 (CH), 49.8 (t, $^1J_{C,F}$ = 26.0, C) ppm; **IR: $\tilde{v}$** = 3351 (vs, N–H) cm^{-1}; **HRMS-ESI:** calcd. for $C_{10}H_8ClF_2N_2$ [M–H]$^-$: 229.0350. Found: 229.0351.

4.7.6. *5-(Dichloromethyl)dipyrromethane (3e)*

Procedure B: to a solution of 2-(dichloroacetyl)-pyrrole **5e** (272 mg, 1.53 mmol, 1 equiv.) and NaHCO$_3$ (257 mg, 3.06 mmol, 2 equiv.) suspended in methanol (4.6 mL) under firm stirring was added NaBH$_4$ (116 mg, 3.06 mmol, 2 equiv.) by portions. The mixture was stirred at room temperature for 30 min before removal of the solvent by evaporation. The crude product was dissolved in Et$_2$O. This organic phase

was washed with water, dried over Na$_2$SO$_4$ and evaporated at 30 °C. The resulting solid was then dissolved in pyrrole (0.21 mL, 3.06 mmol, 2 equiv.) before the addition of an aqueous HCl solution (0.18 M, 5 mL). The mixture was stirred at room temperature for 16 h. The mixture was then extracted with CH$_2$Cl$_2$. The organic phase was washed with water, dried on Na$_2$SO$_4$ and evaporated to dryness. The final purification by flash chromatography (CH$_2$Cl$_2$/petroleum ether 2:1) afforded **3e** as a gray solid (212 mg, 0.9 mmol, 60%). **Scale up:** the same procedure at a ten-fold larger scale starting from **5e** (2.72 g, 15.3 mmol) afforded **3e** as a white solid (2.37 g, 10.3 mmol, 67%).

R$_F$ = 0.4 (silica, CH$_2$Cl$_2$/petroleum ether 2:1). **Mp:** > 60 °C (degradation) **^{1}H NMR (CDCl$_3$) δ** = 8.26 (br s, 2H, NH), 6.75 (m, 2H, α-H), 6.25 (m, 2H, β-H), 6.21 (m, 3H, β-H and CHCl$_2$), 4.83 (d, $^3J_{H,H}$ = 3.5, 1H, *meso*-H) ppm; **^{13}C {^{1}H} NMR (CDCl$_3$) δ** = 126.8 (C), 118.3 (CH), 108.8 (CH), 108.7 (CH), 74.9 (CH), 49.0 (CH) ppm; **IR: $\tilde{v}$** = 3344 (vs, N–H), 742 (vs, C–Cl) cm^{-1}; **HRMS-ESI:** calcd. for $C_{10}H_8Cl_2N_4$ [M–H]$^-$: 227.0148. Found: 227.0151.

4.7.7. *5-(Trichloromethyl)dipyrromethane (3f)*

Procedure C: to a solution of 2-(trichloroacetyl)-pyrrole **5f** (1.63 g, 7.7 mmol, 1 equiv.) and NaHCO$_3$ (1.28 g, 15.3 mmol, 2 equiv.) suspended in methanol (23 mL) under firm stirring was added NaBH$_4$ (581 mg, 15.3 mmol, 2 equiv.) by portions. The mixture was stirred at room temperature for 30 min before removal of the solvent by evaporation. The crude product was dissolved in Et$_2$O. This organic phase was washed with water, dried over Na$_2$SO$_4$ and evaporated at 30 °C. The resulting solid and pyrrole (6.0 mL, 86 mmol, 11 equiv.) were dissolved in distilled THF (40 mL) under argon atmosphere before the addition of a solution of HCl in Et$_2$O (1 M, 6.9 mL, 6.9 mmol, 0.9 equiv.). The mixture was stirred at 85 °C for 2 h, quenched with a saturated aqueous NaHCO$_3$ solution. The mixture was extracted by diethyl ether. The organic phase was washed with water, dried over Na$_2$SO$_4$ and evaporated to dryness. The final purification by flash chromatography (CH$_2$Cl$_2$/petroleum ether 2:1) afforded **3f** as a white solid (181 mg, 0.68 mmol, 9%).

R$_F$ = 0.45 (silica, CH$_2$Cl$_2$/petroleum ether 2:1). **Mp:** > 70 °C (decomposition); **^{1}H NMR (CDCl$_3$) δ** = 8.38 (br s, 2H, NH), 6.78 (s, 2H, α-H), 6.41 (s, 2H, β-H), 6.23 (s, 2H, β-H), 5.16 (s, 1H, *meso*-H) ppm; **^{13}C**

{^{1}H} NMR (CDCl$_3$) δ = 126.3 (C), 118.3 (CH), 110.2 (CH), 108.8 (CH), 59.2 (CH), 31.0 (C) ppm; **IR: v~** = 3340 (s, N–H), 741 (vs, C–Cl) cm^{-1}; **HMRS-ESI:** calcd. for C$_{10}$H$_{10}$Cl$_3$N$_2$ [M+H]$^+$: 262.9904. Found: 262.9899.

4.7.8. *5,15-Bis(trifluoromethyl)-10,20-bis-(4-methoxyphenyl)porphyrin (6a)*

Under argon, to a solution of 5-(trifluoromethyl)-dipyrromethane **3a** (643 mg, 3 mmol, 1 equiv.) and 4-methoxybenzaldehyde (0.36 mL, 3 mmol, 1 equiv.) in CH$_2$Cl$_2$ (300 mL) was added BF$_3$·OEt$_2$ (2.5 M, 0.4 mL, 1 mmol, 0.33 equiv.). The mixture was stirred at room temperature for 4 h before DDQ (1.01 g, 4.5 mmol, 1.5 equiv.) was added and the stirring maintained for 10 min. The mixture was passed over a short silica gel plug (CH$_2$Cl$_2$/petroleum ether 1:2). The following purification by flash chromatography (CH$_2$Cl$_2$/petroleum ether 1:4) afforded **6a** as a dark purple solid (88 mg, 0.13 mmol, 9%).

R$_F$ = 0.15 (silica, CH$_2$Cl$_2$/petroleum ether 1:4). ^{1}**H NMR (CDCl$_3$)** δ = 9.59 (m, 4H, β-H), 8.93 (d, $^3J_{H,H}$ = 5.0, 4H, β-H), 8.06 (d, $^3J_{H,H}$ = 8.4, 4H, Ar–H), 7.31 (d, $^3J_{H,H}$ = 8.4, 4H, Ar–H), 4.13 (s, 6H, CH$_3$), −2.64 (br s, 2H, NH) ppm; ^{19}**F NMR (CDCl$_3$)** δ = −37.0, −45.5 ppm; ^{13}**C {^{1}H} NMR (CDCl$_3$)** δ = 160.0 (C), 135.6 (CH), 134.3 (C), 133.8 (CH), 130.0 (CH), 128.1 (d, $^1J_{C,F}$ = 275, C), 122.0 (C), 112.5 (CH), 105.5 (d, $^2J_{C,F}$ = 30.5, C), 55.8 (CH), 53.6 (CH), 29.9 (CH$_3$) ppm; **IR: v~** = 3299.2 (w, N–H), 2918.7, 2843.1 (m, C$_\beta$-H) cm^{-1}; **UV–Vis (CH$_2$Cl$_2$):** λ_{max} (ε) = 416.0 (180 530), 514.1 (10 730), 550.0 (8 490), 594.9 (4 300), 648.0 nm (7220 mol^{-1}·L·cm^{-1}); **Fluorescence (CH$_2$Cl$_2$):** λ_{ex} = 590 nm, λ_{em} = 656, 722 nm; **HRMS-ESI:** calcd. for C$_{36}$H$_{25}$F$_6$N$_4$O$_2$ [M+H]$^+$: 659.1876. Found: 659.1877.

4.7.9. *5,15-Bis(perfluoropropyl)-10,20-bis-(4-methoxyphenyl)porphyrin (6b)*

A solution of 5-(perfluoropropyl)dipyrromethane **3b** (471 mg, 1.5 mmol, 1 equiv.) and 4-methoxy-benzaldehyde (0.18 mL, 1.5 mmol, 1 equiv.) in CH$_2$Cl$_2$ (300 mL) was stirred under argon before the addition of TFA (1.16 mL, 15.1 mmol, 10 equiv.). The mixture was stirred at room temperature for 4 h before DDQ (570 mg, 2.25 mmol, 1.5 equiv.) was added. The resulting mixture was stirred for 16 h before being passed over a short silica gel plug (CH$_2$Cl$_2$/petroleum ether 1:2). The following purification by flash chromatography (CH$_2$Cl$_2$/petroleum

ether 1:4) afforded **6b** as a dark purple solid (29 mg, 0.03 mmol, 4.5%).

R$_F$ = 0.25 (silica, CH$_2$Cl$_2$/petroleum ether 1:4). ^{1}**H NMR (CDCl$_3$)** δ = 9.45 (br s, 4H, β-H), 8.94 (d, $^3J_{H,H}$ = 5.1, 4H, β-H), 8.07 (d, $^3J_{H,H}$ = 7.1, 4H, Ar–H), 7.31 (d, $^3J_{H,H}$ = 8.6, 4H, Ar–H), 4.13 (s, 6H, CH$_3$), −2.53 (br s, 2H, NH) ppm; ^{19}**F NMR (CDCl$_3$)** δ = −76.1 (CF$_3$), −81.8, −119.9 ppm; ^{13}**C {^{1}H} NMR** spectra could not be obtained due to the poor solubility in deuterated solvents; **IR: v~** = 3271.6 (w, N–H) cm^{-1}; **UV–Vis (CH$_2$Cl$_2$):** λ_{max} (ε) = 414 (189,000), 514 (9910), 551 (11,430), 595 (4640), 646 nm (10,655 mol^{-1}·L·cm^{-1}); **Fluorescence (CH$_2$Cl$_2$):** λ_{ex} = 590 nm, λ_{em} = 656, 719 nm; **HRMS-ESI:** calcd. for C$_{48}$H$_{23}$F$_{30}$N$_4$O$_2$ [M–H]$^-$: 857.1603. Found: 857.1602.

4.7.10. *5,15-Bis(perfluoroheptyl)-10,20-bis-(4-methoxyphenyl)porphyrin (6c)*

A solution of 5-(perfluoroheptyl)dipyrromethane **3c** (771 mg, 1.5 mmol, 1 equiv.) and 4-methoxy-benzaldehyde (0.18 mL, 1.5 mmol, 1 equiv.) in CH$_2$Cl$_2$ (300 mL) was stirred under argon before the addition of TFA (1.16 mL, 15.1 mmol, 10 equiv.). The mixture was stirred at room temperature for 4 h before DDQ (570 mg, 2.25 mmol, 1.5 equiv.) was added and the stirring maintained for 16 h. The mixture was passed over a short silica gel plug (CH$_2$Cl$_2$/petroleum ether 1:2). The following purification by flash chromatography (CH$_2$Cl$_2$/petroleum ether 1:4) afforded **6c** as a dark purple solid (37 mg, 0.03 mmol, 4%).

R$_F$ = 0.4 (silica, CH$_2$Cl$_2$/petroleum ether 1:4); ^{1}**H NMR (CDCl$_3$)** δ = 9.45 (br s, 4H, β-H), 8.94 (d, $^3J_{H,H}$ = 5.1, 4H, β-H), 8.07 (br s, 4H, Ar–H), 7.31 (d, $^3J_{H,H}$ = 8.4, 4H, Ar–H), 4.13 (s, 6H, CH$_3$), −2.52 (br s, 2H, NH) ppm; ^{19}**F NMR (CDCl$_3$)** δ = −80.5 (CF$_3$), −81.1, −115.1, −120.7, −121.4, −122.3, −125.9 ppm; ^{13}**C {^{1}H} NMR** spectra could not be obtained due to the poor solubility in deuterated solvents; **IR: v~** = 2958, 2922, 2854 (s, C$_\beta$-H) cm^{-1}; **UV–Vis (CH$_2$Cl$_2$):** λ_{max} (ε) = 415 (198,140), 514 (10,420), 552 (12,680), 596 (5070), 647 nm (10,610 mol^{-1}·L·cm^{-1}); **Fluorescence (CH$_2$Cl$_2$):** λ_{ex} = 590 nm, λ_{em} = 655, 720 nm; **HRMS-ESI:** calcd for C$_{40}$H$_{23}$F$_{14}$N$_4$O$_2$ [M–H]$^-$: 1257.1347. Found: 1257.1349.

4.7.11. *5,15-Bis(fluoroacyl)-10,20-bis-(4-methoxyphenyl)porphyrin (6d)*

A solution of 5-(chlorodifluoromethyl)dipyrromethane **3d** (345 mg, 1.5 mmol, 1 equiv.) and 4-methoxybenzaldehyde (0.18 mL, 1.5 mmol, 1 equiv.) in CH_2Cl_2 (150 mL) was stirred under argon before the addition of $BF_3 \cdot O(Et)_2$ (2.5 M, 0.2 mL, 0.5 mmol, 0.33 equiv.). The mixture was stirred at room temperature for 4 h before DDQ (510 mg, 4.5 mmol, 1.5 equiv.) was added and the stirring maintained for 10 min. The crude product was passed over a short silica gel plug (CH_2Cl_2). The following purification by flash chromatography (CH_2Cl_2/petroleum ether 1:1 then 2:1) afforded **6d** as a dark purple solid (7 mg, 15 μmol, < 2%).

R_F = 0.6 (silica, CH_2Cl_2/petroleum ether 2:1). **¹H NMR (CDCl₃) δ** = 9.61 (m, 4H, β-H), 9.01 (d, $^3J_{H,H}$ = 4.9, 4H, β-H), 8.09 (d, $^3J_{H,H}$ = 8.5, 4H, Ar–H), 7.34 (d, $^3J_{H,H}$ = 8.5, 4H, Ar–H), 4.13 (s, 6H, CH₃), −2.68 (br s, 2H, NH) ppm; **¹⁹F NMR (CDCl₃) δ** = −67.62 ppm; **¹³C {¹H} NMR** spectra could not be obtained due to little quantity; **IR: v~** = 2921, 2853 (vs, C$_\beta$-H) cm⁻¹; **UV–Vis (CH₂Cl₂): λ_{max} (ε)** = 419 (204,600), 521 (9650), 564 (11,780), 663 nm (11,290 mol⁻¹·L·cm⁻¹); **Fluorescence (CH₂Cl₂):** λ_{ex} = 590 nm, λ_{em} = 690 nm; **HRMS-ESI:** calcd. for $C_{36}H_{25}N_4O_4F_2$ [M+H]⁺: 615.1838. Found: 615.1838.

4.7.12. *5,15-Bis(formyl)-10,20-bis-(4-methoxyphenyl)porphyrin (6e)*

A solution of 5-(dichloromethyl)dipyrromethane **3e** (230 mg, 1 mmol, 1 equiv.) and 4-methoxybenzaldehyde (0.12 mL, 1 mmol, 1 equiv.) in CH_2Cl_2 (200 mL) was stirred under argon before the addition of TFA (0.77 mL, 10 mmol, 10 equiv.). The mixture was stirred at room temperature for 4 h before DDQ (340 mg, 1.5 mmol, 1.5 equiv.) and the stirring maintained for 16 h. The mixture was passed over a short silica gel plug (CH_2Cl_2/AcOEt 9:1). The following purification by flash chromatography (CH_2Cl_2, then CH_2Cl_2/AcOEt 2.5%) afforded **6e** as a dark purple solid (31 mg, 0.05 mmol, 11%).

R_F = 0.6 (silica, CH_2Cl_2/AcOEt 97.5:2.5). **¹H NMR (CDCl₃) δ** = 12.53 (s, 2H, CHO), 10.01 (d, $^3J_{H,H}$ = 4.8, 4H, β-H), 9.01 (d, $^3J_{H,H}$ = 4.8, 4H, β-H), 8.08 (d, $^3J_{H,H}$ = 8.5, 4H, Ar–H), 7.33 (d, $^3J_{H,H}$ = 8.5, 4H, Ar–H), 4.13 (s, 6H, CH₃), −2.30 (br s, 2H, NH) ppm; **¹³C {¹H} NMR** spectra could not be obtained due

to the poor solubility in deuterated solvents; **IR: v~** = 3318 (w, N–H), 2957, 2921, 2852 (m, C$_\beta$-H), 1672 (vs, C=O) cm⁻¹; **UV–Vis (CH₂Cl₂): λ_{max} (ε)** = 430 (193,270), 510 (4040), 538 (6900), 587 (17,130), 686 nm (14,880 mol⁻¹·L·cm⁻¹); **Fluorescence (CH₂Cl₂):** λ_{ex} = 590 nm, λ_{em} = 707, 771 nm; **HRMS-ESI:** calcd. for $C_{36}H_{27}N_4O_4$ [M+H]⁺: 579.2027. Found: 579.2031.

4.7.13. *5,15-Bis(formyl)-10,20-bis-(4-cyanophenyl)porphyrin (7)*

A solution of 5-(dichloromethyl)dipyrromethane **3e** (345 mg, 1.5 mmol, 1 equiv.) and 4-cyanobenzaldehyde (197 mg, 1.5 mmol, 1 equiv.) in CH_2Cl_2 (300 mL) was stirred under argon before the addition of TFA (1.15 mL, 15 mmol, 10 equiv.). The mixture was stirred at room temperature for 2 h before DDQ (570 mg, 2.25 mmol, 1.5 equiv.) was added and the stirring maintained for 10 min. The mixture was passed over a short silica gel plug (CH_2Cl_2/AcOEt 9:1). The following purification by flash chromatography (CH_2Cl_2, then CH_2Cl_2/AcOEt 2.5%) afforded **7** as a dark purple solid (39 mg, 0.07 mmol, 9%).

R_F = 0.5 (silica, CH_2Cl_2/AcOEt 97.5:2.5). **¹H NMR (DMSO-d₆, 85 °C) δ** = 12.56 (s, 2H, CHO), 10.19 (d, $^3J_{H,H}$ = 5.1, 4H, β-H), 8.95 (d, $^3J_{H,H}$ = 5.1, 4H, β-H), 8.43 (d, $^3J_{H,H}$ = 8.0, 4H, Ar–H), 8.31 (d, $^3J_{H,H}$ = 8.0, 4H, Ar–H), −2.40 (br s, 2H, NH) ppm; **¹³C {¹H} NMR** spectra could not be obtained due to the poor solubility in deuterated solvents; **IR: v~** = 3316 (w, N–H), 1671 (vs, C=O) cm⁻¹; **UV–Vis (CH₂Cl₂): λ_{max} (ε)** = 427 (102,970), 508 (2250), 535 (3840), 579 (8460), 680 nm (7470 mol⁻¹·L·cm⁻¹); **Fluorescence (CH₂Cl₂):** λ_{ex} = 590 nm, λ_{em} = 688, 757 nm; **HRMS-ESI:** calcd. for $C_{36}H_{21}N_6O_2$ [M+H]⁺: 569.1721. Found: 569.1716.

4.7.14. *5,15-Bis(formyl)-10,20-bis-(4-chlorophenyl)porphyrin (8)*

A solution of 5-(dichloromethyl)dipyrromethane **3e** (345 mg, 1.5 mmol, 1 equiv.) and 4-chlorobenzaldehyde (0.21 mL, 1.5 mmol, 1 equiv.) in CH_2Cl_2 (300 mL) was stirred under argon before the addition of TFA (1.15 mL, 15 mmol, 10 equiv.). The mixture was stirred at room temperature for 2 h before DDQ (570 mg, 2.25 mmol, 1.5 equiv.) was added and the stirring maintained for 10 min. The mixture was passed over a short silica gel plug (CH_2Cl_2/AcOEt 9:1). The following purification by

flash chromatography (CH_2Cl_2) afforded **8** as a dark purple solid (8 mg, 13 µmol, < 2%).

R_F = 0.7 (silica, CH_2Cl_2). **^{1}H NMR (CDCl$_3$) δ** = 12.54 (s, 2H, CHO), 10.04 (4H, β-H), 8.97 (d, $^3J_{H,H}$ = 4.9, 4H, β-H), 8.11 (d, $^3J_{H,H}$ = 7.9, 4H, Ar–H), 7.79 (d, $^3J_{H,H}$ = 7.9, 4H, Ar–H), −2.38 (br s, 2H, NH) ppm; **^{13}C {^{1}H} NMR** spectra could not be obtained due to the poor solubility in deuterated solvents; **IR: $\tilde{v}$** = 1671 (vs, C=O) cm^{-1}; **UV–Vis (CH_2Cl_2):** λ_{max} (ε) = 427 (116,900), 535 (3630), 583 (10,310), 682 nm (9140 mol^{-1}·L·cm^{-1}); **Fluorescence (CH_2Cl_2):** λ_{ex} = 590 nm, λ_{em} = 692, 763 nm; **HRMS-ESI:** calcd. for $C_{34}H_{21}Cl_2N_4O_2$ [M+H]$^+$: 587.1036. Found: 587.1038.

4.7.15. *5,15-Bis(formyl)-10,20-bis-(4-tert-butylphenyl)porphyrin (9)*

A solution of 5-(dichloromethyl)dipyrromethane **3e** (173 mg, 0.75 mmol, 1 equiv.) and 4-*tert*-butylbenzaldehyde (0.13 mL, 0.75 mmol, 1 equiv.) in CH_2Cl_2 (150 mL) was stirred under argon before the addition of TFA (0.58 mL, 7.5 mmol, 10 equiv.). The mixture was stirred at room temperature for 2 h before DDQ (285 mg, 1.13 mmol, 1.5 equiv.) was added and the stirring maintained for 10 min. The mixture was passed over a short silica gel plug (CH_2Cl_2/AcOEt 9:1). The following purification by flash chromatography (CH_2Cl_2, then CH_2Cl_2/AcOEt 2.5%) afforded **9** as a dark purple solid (29 mg, 0.045 mmol, 12%).

R_F = 0.8 (silica, CH_2Cl_2). **^{1}H NMR (CDCl$_3$) δ** = 12.51 (s, 2H, CHO), 9.98 (d, $^3J_{H,H}$ = 4.8, 4H, β-H), 9.00 (d, $^3J_{H,H}$ = 4.8, 4H, β-H), 8.09 (d, $^3J_{H,H}$ = 8.1, 4H, Ar–H), 7.81 (d, $^3J_{H,H}$ = 8.1, 4H, Ar–H), 1.64 (s, 18H, tertbutyl-H), −2.37 (br s, 2H, NH) ppm; **^{13}C {^{1}H} NMR** spectra could not be obtained due to the poor solubility in deuterated solvents; **IR: $\tilde{v}$** = 3302 (vw, N–H), 2962 (w, C$_\beta$-H), 1671 (vs, C=O) cm^{-1}; **UV–Vis (CH_2Cl_2):** λ_{max} (ε) = 427 (206,460), 539 (6160), 585 (17,490), 684 nm (15,410 mol^{-1}·L·cm^{-1}); **Fluorescence (CH_2Cl_2):** λ_{ex} = 590 nm, λ_{em} = 696, 767 nm; **HRMS-ESI:** calcd. for $C_{42}H_{39}N_4O_2$ [M+H]$^+$: 631.3068. Found: 631.3068.

Acknowledgments

Supplementary data

Supporting information for this article is available on the journal's website under https://doi.org/10.5802/crchim.97 or from the author.

The document contains ^{1}H, ^{19}F and ^{13}C NMR spectra, additional cyclic voltammograms, absorption and emission spectra, additional theoretical details.

References

[1] K. M. Kadish, K. M. Smith, R. Guilard (eds.), *The Porphyrin Handbook*, vol. 1–10, Academic Press, San Diego, 2000.

[2] K. M. Kadish, K. M. Smith, R. Guilard (eds.), *The Porphyrin Handbook*, vol. 11–20, Academic Press, San Diego, 2003.

[3] K. M. Kadish, K. M. Smith, R. Guilard (eds.), *Handbook of Porphyrin Science*, vol. 1–10, World Scientific Publishing, Singapore, 2010.

[4] K. M. Kadish, K. M. Smith, R. Guilard (eds.), *Handbook of Porphyrin Science*, vol. 11–15, World Scientific Publishing, Singapore, 2011.

[5] K. M. Kadish, K. M. Smith, R. Guilard (eds.), *Handbook of Porphyrin Science*, vol. 16–25, World Scientific Publishing, Singapore, 2012.

[6] Y. Inokuma, A. Osuka, *Dalton Trans.*, 2008, 2517-2526.

[7] T. Tanaka, A. Osuka, *Chem. Rev.*, 2017, **117**, 2584-2640.

[8] R. Orłowski, D. Gryko, D. T. Gryko, *Chem. Rev.*, 2017, **117**, 3102-3137.

[9] J. K. Laha, S. Dhanalekshmi, M. Taniguchi, A. Ambroise, J. S. Lindsey, *Org. Process Res. Dev.*, 2003, **7**, 799-812.

[10] D. T. Gryko, D. Gryko, C.-H. Lee, *Chem. Soc. Rev.*, 2012, **41**, 3780-3789.

[11] N. A. M. Pereira, T. M. V. D. Pinho e Melo, *Org. Prep. Proced. Int.*, 2014, **46**, 183-213.

[12] B. F. O. Nascimento, S. M. M. Lopes, M. Pineiro, T. M. V. D. Pinho e Melo, *Molecules*, 2019, **24**, article no. 4348.

[13] T. P. Wijesekera, *Can. J. Chem.*, 1996, **74**, 1868-1871.

[14] S. L. Gould, G. Kodis, R. E. Palacios, L. de la Garza, A. Brune, D. Gust, T. A. Moore, A. L. Moore, *J. Phys. Chem. B*, 2004, **108**, 10566-10580.

[15] L. Li, B. Nguyen, K. Burgess, *Bioorg. Med. Chem. Lett.*, 2008, **18**, 3112-3116.

[16] A. Nayak, J. Park, K. De Mey, X. Hu, T. V. Duncan, D. N. Beratan, K. Clays, M. J. Therien, *ACS Cent. Sci.*, 2016, **2**, 954-966.

[17] A. Nayak, S. Roy, B. D. Sherman, L. Alibabaei, A. M. Lapides, M. K. Brennaman, K.-R. Wee, T. J. Meyer, *ACS Appl. Mater. Interfaces*, 2016, **8**, 3853-3860.

[18] A. Osuka, G. Noya, S. Taniguchi, T. Okada, Y. Nishimura, I. Yamazaki, N. Mataga, *Chem. Eur. J.*, 2000, **6**, 33-46.

[19] N. Nishino, R. W. Wagner, J. S. Lindsey, *J. Org. Chem.*, 1996, **61**, 7534-7544.

[20] R. Goldschmidt, I. Goldberg, Y. Balazs, Z. Gross, *J. Porphyr. Phthalocyanines*, 2006, **10**, 76-86.

[21] W. Dmowski, K. Piasecka-Maciejewska, Z. Urbanczyk-Lipkowska, *Synthesis*, 2003, 841-844.

[22] W. Dmowski, K. Piasecka-Maciejewska, Z. Urbańczyk-Lipkowska, *Kem. Ind.*, 2004, **53**, 339-341.

[23] A. K. Wertsching, A. S. Koch, S. G. DiMagno, *J. Am. Chem. Soc.*, 2001, **123**, 3932-3939.

[24] B. E. Smart, *J. Fluor. Chem.*, 2001, **109**, 3-11.

[25] A. Rivkin, K. Biswas, T.-C. Chou, S. J. Danishefsky, *Org. Lett.*, 2002, **4**, 4081-4084.

[26] S. G. DiMagno, R. A. Williams, M. J. Therien, *J. Org. Chem.*, 1994, **59**, 6943-6948.

[27] S. G. DiMagno, A. K. Wertsching, C. R. Ross, *J. Am. Chem. Soc.*, 1995, **117**, 8279-8280.

[28] K. E. Thomas, J. Conradie, L. K. Hansen, A. Ghosh, *Inorg. Chem.*, 2011, **50**, 3247-3251.

[29] K. T. Moore, J. T. Fletcher, M. J. Therien, *J. Am. Chem. Soc.*, 1999, **121**, 5196-5209.

[30] S. G. DiMagno, P. H. Dussault, J. A. Schultz, *J. Am. Chem. Soc.*, 1996, **118**, 5312-5313.

[31] T. S. Balaban, A. D. Bhise, M. Fischer, M. Linke-Schaetzel, C. Roussel, N. Vanthuyne, *Angew. Chem. Int. Ed.*, 2003, **42**, 2140-2144.

[32] N. Sugita, S. Hayashi, F. Hino, T. Takanami, *J. Org. Chem.*, 2012, **77**, 10488-10497.

[33] M. O. Senge, S. S. Hatscher, A. Wiehe, K. Dahms, A. Kelling, *J. Am. Chem. Soc.*, 2004, **126**, 13634-13635.

[34] A. Balakumar, K. Muthukumaran, J. S. Lindsey, *J. Org. Chem.*, 2004, **69**, 5112-5115.

[35] L. N. Sobenina, A. M. Vasil'tsov, O. V. Petrova, K. B. Petrushenko, I. A. Ushakov, G. Clavier, R. Meallet-Renault, A. I. Mikhaleva, B. A. Trofimov, *Org. Lett.*, 2011, **13**, 2524-2527.

[36] V. Král, P. Vašek, B. Dolenský, *Collect. Czech. Chem. Commun.*, 2004, **69**, 1126-1136.

[37] A. J. F. N. Sobral, N. G. C. L. Rebanda, M. da Silva, S. H. Lampreia, M. Ramos Silva, A. M. Beja, J. A. Paixão, A. M. d. A. Rocha Gonsalves, *Tetrahedron Lett.*, 2003, **44**, 3971-3973.

[38] M. Bagherzadeh, M. A. Jonaghani, M. Amini, A. Mortazavi-Manesh, *J. Porphyr. Phthalocyanines*, 2019, **23**, 671-678.

[39] T. Rohand, E. Dolusic, T. H. Ngo, W. Maes, W. Dehaen, *ARKIVOC*, 2007, 307-324.

[40] H. Falk, H. Wöss, *Monatsh. Chem.*, 1988, **119**, 1031-1035.

[41] S. Shimizu, N. Aratani, A. Osuka, *Chem. Eur. J.*, 2006, **12**, 4909-4918.

[42] S.-J. Hong, M.-H. Lee, C.-H. Lee, *Bull. Korean Chem. Soc.*, 2004, **25**, 1545-1550.

[43] R. Paolesse, L. Jaquinod, M. O. Senge, K. M. Smith, *J. Org. Chem.*, 1997, **62**, 6193-6198.

[44] W. Schwertfeger, G. Siegemund, *J. Fluor. Chem.*, 1987, **36**, 237-246.

[45] A. Wickramasinghe, L. Jaquinod, D. J. Nurco, K. M. Smith, *Tetrahedron*, 2001, **57**, 4261-4269.

[46] M. Suzuki, S. Neya, Y. Nishigaichi, *Molecules*, 2016, **21**, article no. 252.

[47] A. Nemes, E. Mérész, I. Jalsovszky, D. Szabó, Z. Böcskei, J. Rábai, *J. Fluor. Chem.*, 2017, **203**, 75-80.

[48] L. Chen, L.-M. Jin, C.-C. Guo, Q.-Y. Chen, *Synlett*, 2005, 963-970.

[49] Z. Zeng, C. Liu, L.-M. Jin, C.-C. Guo, Q.-Y. Chen, *Eur. J. Org. Chem.*, 2005, 306-316.

[50] K. S. F. Lau, M. Sadilek, G. E. Khalil, M. Gouterman, C. Brückner, *J. Am. Soc. Mass. Spectrom.*, 2005, **16**, 1915-1920.

[51] J. G. Goll, K. T. Moore, A. Ghosh, M. J. Therien, *J. Am. Chem. Soc.*, 1996, **118**, 8344-8354.

[52] C. Hansch, A. Leo, R. W. Taft, *Chem. Rev.*, 1991, **91**, 165-195.

[53] J. C. P. Grancho, M. M. Pereira, M. d. G. Miguel, A. M. R. Gonsalves, H. D. Burrows, *Photochem. Photobiol.*, 2002, **75**, 249-256.

[54] A. M. Brouwer, *Pure Appl. Chem.*, 2011, **83**, 2213-2228.

[55] N. G. Connelly, W. E. Geiger, *Chem. Rev.*, 1996, **96**, 877-910.

[56] M. J. Frisch *et al.*, "GAUSSIAN 16 Revision C.01", 2016, Gaussian Inc. Wallingford CT.

[57] D. Jacquemin, V. Wathelet, E. A. Perpète, C. Adamo, *J. Chem. Theory Comput.*, 2009, **5**, 2420-2435.

[58] A. D. Laurent, D. Jacquemin, *Int. J. Quantum Chem.*, 2013, **113**, 2019-2039.

[59] V. Barone, M. Cossi, *J. Phys. Chem. A*, 1998, **102**, 1995-2001.

[60] B. Miehlich, A. Savin, H. Stoll, H. Preuss, *Chem. Phys. Lett.*, 1989, **157**, 200-206.

[61] O. V. Dolomanov, L. J. Bourhis, R. J. Gildea, J. A. K. Howard, H. Puschmann, *J. Appl. Crystallogr.*, 2009, **42**, 339-341.

[62] G. M. Sheldrick, *Acta Crystallogr.*, 2015, **C71**, 3-8.

[63] W. J. Peláez, M. A. Burgos Paci, G. A. Argüello, *Tetrahedron Lett.*, 2009, **50**, 1934-1938.

[64] J. Rábai, A. Nemes, I. Jalsovszky, D. Szabó, *Fluorine Notes*, 2016, **104**, 1-7.

[65] Y. Çetinkaya, M. Balci, *Tetrahedron Lett.*, 2014, **55**, 6698-6702.

[66] A. T. Dubis, M. Domagała, S. J. Grabowski, *New J. Chem.*, 2010, **34**, 556-566.

[67] A. A. Ribeiro, *Magn. Reson. Chem.*, 1997, **35**, 215-221.